Progress in Oceanography 209 (2022) 102908

Contents lists available at ScienceDirect

Progress in Oceanography

journal homepage: www.elsevier.com/locate/pocean

Climatology and process-oriented analysis of the Adriatic sea level extremes

Jadranka Šepić [a,*], Miroslava Pasarić [b], Iva Međugorac [b], Ivica Vilibić [c,d], Maja Karlović [e], Marko Mlinar [e]

[a] Faculty of Science, University of Split, R. Boškovića 33, 21000 Split, Croatia
[b] Department of Geophysics, Faculty of Science, University of Zagreb, Horvatovac 95, 10000 Zagreb, Croatia
[c] Ruđer Bošković Institute, Division for Marine and Environmental Research, Bijenička cesta 54, 10000 Zagreb, Croatia
[d] Institute of Oceanography and Fisheries, Šetalište I. Meštrovića 63, 21000 Split, Croatia
[e] Hydrographic Institute of the Republic of Croatia, Zrinsko-Frankopanska 161, Split, Croatia

A B S T R A C T

The strongest episodes of extremely high sea levels in the Mediterranean are regularly observed in the Adriatic Sea, where they can cause substantial damage and loss of human lives. In this study, episodes of positive and negative sea level extremes were extracted from hourly series measured at six tide gauge stations located along the Adriatic coast (Venice, Trieste, Rovinj, Bakar, Split, Dubrovnik) between 1956 and 2019/2020. The time series were first checked for spurious data and then decomposed using tidal analysis, least-squares fitting and filtering procedures into (1) *trend*; (2) *seasonal*; (3) *tide*, (4) longer than 100 d (> 100 *d*), (5) 10–100 *d*, (6) 6 *h*-10 *d*, and (7) < 6 *h components*. These components correspond to sea level oscillations dominantly (but not exclusively) forced by (1) climate and isostatic change; (2) seasonal changes in thermohaline properties and circulation patterns, (3) tidal forcing, (4) quasi-stationary atmospheric and ocean circulation and climate variability patterns, (5) planetary atmospheric waves, (6) synoptic, and (7) mesoscale atmospheric processes.

Significant differences exist between (1) the northern and middle/southern Adriatic extremes and (2) positive and negative extremes. The heights and return levels of positive (negative) extremes are 50–100% higher (lower) in the northern than in the middle/southern Adriatic. The northern Adriatic positive sea level extremes dominantly occur due to the superposition of the 6 *h*-10 *d component* and *tide* (contributing jointly to ~70% of the total extreme height), whereas the middle/southern Adriatic positive extremes mostly occur due to the superposition of the 10–100 *d component*, 6 *h*-10 *d component*, and *tide* (each contributing ~25% on average). The negative sea level extremes are explained as a combination of the 10–100 *d* component and tide: in the northern Adriatic tide provides the largest contribution (~60%), while in the middle/southern Adriatic, the impacts of the two processes are similar (each contributing an average of ~30%). Over the entire Adriatic, the < 6 *h* and *seasonal components* contribute the least to both positive and negative extremes. Sea level trends at all stations are positive; however, the observed sea level rise did not contribute significantly to the total height of extremes. Extreme episodes tend to occur simultaneously over larger parts of the coast and are often clustered within a few days. Both positive and negative extremes have a strong decadal variability, whereas trends of their number, duration and intensity point to shortening of negative extremes and prolonging and strengthening of positive extremes.

1. Introduction

Positive sea level extremes are one of the major hazards for coastal regions of world seas (Neumann et al., 2015) and are especially dangerous at coasts that are regularly exposed to severe atmospheric phenomena, such as hurricanes and extratropical cyclones (Mousavi et al., 2011; Hinkel et al., 2015; Enriquez et al., 2020). Negative sea level extremes are researched sporadically (Campetella et al., 2007; Wicks and Atkinson, 2017) – likely because they are not as destructive as positive extremes, which can, during extraordinary events, cause tens to hundreds of thousands of deaths (Kânoğlu et al., 2015; Bouwer and Jonkman, 2018). Sea level extremes are driven by a variety of atmospheric, ocean, hydrological and geological processes, occurring on time scales from minute to millennial and on spatial scales from several kilometres to global. On the global scale, an increase in the strength and frequency of positive sea level extremes has been observed during the 20th and 21st centuries, mainly due to the worldwide mean sea level rise (Menéndez and Woodworth, 2010; Hamlington et al., 2020). On shorter periods, from weeks to years, numerous processes contribute to the slow sea level variability (Leuliette, 2015) and indirectly to sea level extremes. These are circulation patterns (Suzuki and Tatebe, 2020), water balance (evaporation minus precipitation) at the sea surface (Wenzel and Schroter, 2007), and propagation patterns of atmospheric planetary waves (Fukumori et al., 1998). On temporal scales from a few hours up to a few days and on regional and local spatial scales, positive sea level extremes are mostly driven by tropical storms, tropical cyclones (Marsooli et al., 2019), and extratropical cyclones (Enriquez et al., 2020), while negative sea level extremes are driven by anticyclonic activity

* Corresponding author.
E-mail address: jsepic@pmfst.hr (J. Šepić).

https://doi.org/10.1016/j.pocean.2022.102908
Received 29 October 2021; Received in revised form 27 September 2022; Accepted 9 October 2022
Available online 14 October 2022

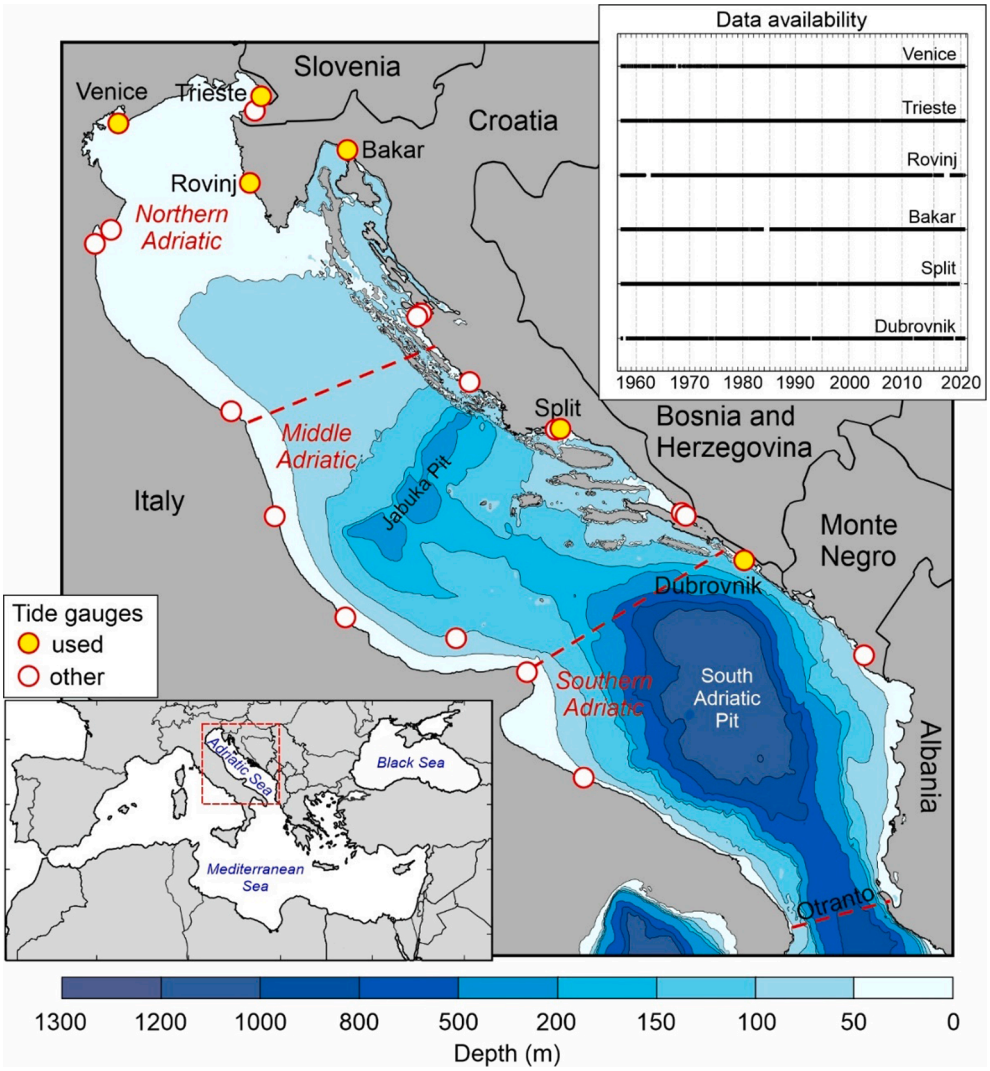

Fig. 1. Map and bathymetry of the Adriatic Sea. The positions of tide gauge stations operational at the end of 2020 are marked with circles; yellow circles mark tide gauges that were selected for the study; white circles mark other tide gauges. Red dashed lines mark borders of the northern, middle and southern Adriatic. The position of the Adriatic Sea relative to the Mediterranean Sea is shown in the small inset in the bottom left corner, and the availability of the time series is shown in the upper right corner. (For interpretation of the references to colour in this figure legend, the reader is referred to the web version of this article.)

(Crisciani et al., 1994) and strong offshore winds (Campetella et al., 2007). Tides, ranging up to > 10 m where they are strongest (Pugh and Woodworth, 2014), represent another significant contributor to the positive and negative sea level extremes. Finally, sea level extremes can also be related to high-frequency sea level phenomena occurring at periods from minutes to hours. The strongest and most destructive of these are tsunamis (Pugh and Woodworth, 2014), but there are others such as atmospherically generated seiches (Woodworth, 2017), meteotsunamis (Rabinovich, 2020), edge waves (Munk et al., 1956; Yankovsky, 2009), infragravity waves (Henderson and Bowen, 2003; Aucan and Ardhuin, 2013) and wind-driven waves (Dodet et al., 2019). Such high-frequency sea level oscillations of nonseismic origin, e.g., seiches and meteotsunamis, are particularly relevant in low-tidal basins (Vilibić and Šepić, 2017), such as the Mediterranean Sea, where they can reach heights comparable and even larger than those observed during the most extreme storm surge events. Most of the abovementioned processes are reflected in the Adriatic sea levels and therefore influence the Adriatic sea level extremes.

The Adriatic Sea is an ~800 km long and ~200 km wide northern embayment of the Mediterranean Sea. The Adriatic can be roughly divided into three parts (Fig. 1): (1) the shallow northern Adriatic (depths of < 100 m) spanning from the northernmost Adriatic coast to the ~80 m isobath; (2) the deeper middle Adriatic encompassing Jabuka Pit in the north and stretching up to the northwestern perimeter of the 1200 m deep south Adriatic Pit; and (3) the deep southern Adriatic containing a circular South Adriatic Pit and extending to the Strait of Otranto. Sea level trends estimated for the period starting at the beginning of the continuous instrumental measurements (between 1870 and 1950 s, depending on the station) and ending in the 1980 s range between 0.8 and 1.4 mm/year along most of the eastern Adriatic coast (Vilibić et al., 2017). An exception is Venice, for which larger trends, mostly due to pumping of underground water and the related subsidence, are estimated for this period (2.5 mm/year) (Pirazzoli, 1987; Tosi et al., 2013). During the recent period (starting in 1993), for which both tide gauge and altimetry measurements have been available, the rate of the sea level trend has increased to at least 1.9 mm/year (as estimated from the tide gauge data), with altimetry data revealing trends of up to 3.2 mm/year (Fenoglio-Marc et al., 2012). At periods shorter than mean sea level change (estimated as a linear trend over 30+ years) but longer than 100 d, sea level variability of the Adriatic Sea is coherent in space (Orlić and Pasarić, 2000; Landerer and Volkov, 2013), yet highly changeable in time, with pronounced decadal to bidecadal (Stravisi and Ferraro, 1986; Orlić and Pasarić, 1994, 2000; Unal and Ghil, 1995) and annual to interannual variability (Orlić and Pasarić, 1994, 2000; Unal and Ghil, 1995; Landerer and Volkov, 2013), often related to wider Mediterranean scale sea level oscillations (Landerer and Volkov, 2013) and thermohaline circulation (Fenoglio-Marc et al., 2012). Regarding the seasonal sea level signal, the annual component is estimated to range on average between 3.8 and 4.7 cm, and the semiannual component ranges between 2.4 and 4.0 cm, with a larger range over the northern

Adriatic (Tsimplis and Woodworth, 1994; Vilibić, 2006a). The spatial variability of the seasonal signal might originate from differences in thermohaline properties of the shallow northern Adriatic and deeper southern Adriatic. The northern Adriatic is more strongly influenced by local freshwater discharges (Raicich, 1996) and strong shallow-water wintertime cooling (Mihanović et al., 2013) than the warmer, more saline, and deeper southern Adriatic (Lipizer et al., 2014). The steric effect is also suggested to influence seasonal patterns of coastal flooding and sea level extremes in the Adriatic (Fenoglio-Marc et al., 2006). Going to shorter periods (10–100 d), sea levels induced by atmospheric planetary waves become extremely important for the variability and amplitude of positive sea level extremes (Pasarić et al., 2000; Pasarić and Orlić, 2001; Ferrarin et al., 2021), but other processes can influence it as well. These processes may include rapid thermohaline changes (e.g., driven by river discharges and plume dynamics, e.g., of Po and Albanian rivers), circulation changes (including instabilities and eddies in coastal currents, e.g., Burrage et al., 2009), thermosteric and water budget effects, particularly in coastal regions, during strong bora outbreaks, and other effects (as discussed in Međugorac et al., 2020); however, these contributions must be quantified in future research. The Adriatic storm surges, with the strongest signal at the 1–3 d period, are normally generated by a low-pressure centre over the Gulf of Genoa or the northern Adriatic, accompanied by strong sirocco winds that pile up the water at the closed end of the Adriatic, having the largest amplitudes there (Orlić et al., 1994; Bertotti et al., 2011). Tides, both diurnal and semidiurnal, are also rising in amplitudes towards the northern Adriatic, occasionally surpassing a 1-metre range (Medvedev et al., 2020). Tides and storm surges are recognized as the most important component of the northern Adriatic floods, especially of the well-known "acqua alta" (It. "high water") floods of the city of Venice (Cavaleri et al., 2020). In addition to all other processes, a unique contribution to the Adriatic sea level extremes comes from the Adriatic fundamental seiche, which has a period of ~21.2 h (Cerovečki et al., 1997) and, like the tides and storm surges, the largest amplitude in the northern Adriatic. The combination of large tides, the storm surge effect, and strong fundamental seiche results in the fact that the positive Adriatic sea level extremes and corresponding return levels are by far the largest of the Mediterranean positive sea level extremes (Marcos et al., 2009). Finally, local seiches and meteotsunamis, occurring at periods from a few minutes up to a few hours, are known to strongly contribute to the overall Adriatic extremes, particularly in complex topographical regions (Caloi, 1938; Vilibić and Šepić, 2009; Šepić et al., 2012a; Orlić, 2015; Bubalo et al., 2021).

In summary, the Adriatic sea level extremes are driven by a variety of processes detectable at different temporal and spatial scales. Some of these processes are coherent over the entire basin, while others show substantial spatial variability. The quantification of these processes as seen on the long-term sea level measurements has been just marginally done for the positive extremes, but not for the negative extremes, and not for all the processes. Therefore, the objectives of this study were (1) to identify the general properties of the positive and negative Adriatic sea level extremes; (2) to analyse the general properties of the sea level series decomposed over relevant frequency domains; and (3) to quantify the contributions of the components to the positive and negative sea level extremes. Section 2 presents the data and the methodology. Section 3 documents the overall statistics of the Adriatic sea level extremes and their climatology. In Section 4, the sea level signal is decomposed into components, and their overall statistics are estimated. Section 5 quantifies the contribution of the various sea level components to the total extremes. All findings are discussed in Section 6, while conclusions are listed in Section 7.

2. Data and methods

2.1. Sea level and ERA5 data

Bathymetry of the Adriatic Sea and positions of the tide gauge stations operational at the end of 2020 are shown in Fig. 1. We have chosen stations Venice, Trieste, Rovinj, Bakar, Split and Dubrovnik for our analysis, as sea level has been measured continuously with hourly resolution at these stations for > 60 years. There are at least two more stations that satisfy the length criteria: Koper and Split Marjan (Pérez Gómez et al., 2022). However, due to the proximity of these stations to the stations Trieste and Split used herein, we decided not to use them in the analysis. In addition, there were many more operational stations in Venice Lagoon at the end of 2020 (Pérez Gómez et al., 2022), but we chose to use only data from the Punta Salute station, as it has by far the longest time series, and to plot only this Venice station in the map.

The Venice tide gauge station is operated by Centro Previsioni e Segnalazioni Maree (https://www.comune.venezia.it/it/content/centro-previsioni-e-segnalazioni-maree), and the Trieste tide gauge station is operated by the Institute of Marine Sciences of the National Research Council of Italy (CNR-ISMAR, https://www.ismar.cnr.it). Bakar station (Croatia) is operated by the Department of Geophysics of the Faculty of Science of the University of Zagreb (Međugorac et al., 2022a; Međugorac et al., 2022b) and Rovinj, Split and Dubrovnik stations (Croatia) by the Hydrographic Institute of the Republic of Croatia (HHI, https://www.hhi.hr). All tide gauge stations used in this study were *stilling well* stations. At Trieste, sea level was measured by a mechanical float instrument until 2001 and by a digital float instrument afterwards (Raicich, 2019). At Venice, sea level was also measured by a mechanical float instrument, which was upgraded with a digital instrument in the early 1980s (Zerbini et al., 2017). Other stations (Rovinj, Bakar, Split and Dubrovnik) measure sea level by float sensors (Pérez Gómez et al., 2022): until the early 2000s, only analogue chart-recording instruments were used, and afterwards, analogue and digital instruments were used, with analogue instruments as the main (due to better stability) and digital instruments as backups. Regarding analogue measurements, hourly values were obtained from the tide gauge charts through manual digitization (done continuously by operating agencies throughout the measurement period). For Trieste, Rovinj, Bakar, Venice and Dubrovnik, available hourly sea level time series cover a period from 1 January 1956 to 31 December 2020, and for Split, from 1 January 1956 to 31 December 2019 (Fig. 1). The obtained hourly sea level time series were quality-checked by operating agencies through year-to-year maintenance. However, before proceeding with the analysis, we performed additional quality checks that included a comparison of yearly and monthly means between nearby stations (resulting in the removal of ~2 years of data from the Rovinj time series due to an offset of 8–10 cm from the expected yearly value) and visual checking of the series, looking at each subsequent week separately, identifying spurious-looking data and checking the original tide charts to see if digitization was properly performed. For the studied period, the numbers of missing and removed months (days) were ~11 months for Venice, 11.6 days for Trieste, ~29 months for Rovinj, ~13 months for Bakar, ~2.5 months for Split, and ~16 months for Dubrovnik (data availability periods are shown in Fig. 1).

Using the hourly sea level data, we (1) evaluated the distributions and return periods of the total positive and negative sea level extremes and assessed their characteristics; (2) decomposed the sea level signal into seven components and evaluated the characteristics of these components; and (3) quantified the contributions of all sea level components to the total positive and negative extremes.

In addition, we used the ERA5 global reanalysis (Hersbach et al., 2020) to discuss a link between the observed sea level processes and the atmospheric forcing. For this purpose, we downloaded hourly time series of the mean sea level pressure (MSLP) and of the 10-m wind at the six ERA5 points closest to the tide gauge locations, all for the 1979 to 2020 period. The data (Hersbach et al., 2018) was downloaded from the Copernicus Climate Change Service (C3S) Climate Data Store.

Table 1
Values of total maximum (max), total minimum (min) sea level, 99.99, 99.95, 0.01 and 0.05 percentile values, and number of extracted episodes at each station. In the columns marked with No. Episodes, the average number of episodes per year is given in brackets.

Station	Venice	Trieste	Rovinj	Bakar	Split	Dubrovnik
Max (cm)	167.5	182.7	114.7	111.5	85.4	74.0
99.99 p (cm)	115.6	115.8	94.7	88.4	70.4	63.0
No. HEP episodes	21 (0.3)	31 (0.5)	23 (0.4)	23 (0.4)	15 (0.2)	22 (0.3)
99.95 p (cm)	95.6	98.7	83.7	76.4	61.4	55.9
No. EP episode	103 (1.6)	136 (2.1)	93 (1.5)	102 (1.6)	77 (1.2)	88 (1.4)
Min (cm)	−116.5	−119.2	−97.3	−82.5	−64.6	−61.0
0.01 p (cm)	−99.5	−102.2	−85.3	−69.6	−54.6	−53.0
No. HEN episodes	34 (0.6)	31 (0.5)	30 (0.5)	29 (0.4)	17 (0.3)	16 (0.2)
0.05 p (cm)	−89.5	−92.2	−76.3	−62.3	−47.6	−45.0
No. EN episodes	131 (2.0)	158 (2.4)	127 (2.0)	121 (1.9)	72 (1.1)	83 (1.3)

2.2. Distributions and return periods of extreme values

Return values (highest/lowest sea level expected to be surpassed once in a period, typically 50 years or 100 years) of sea level extremes were estimated according to the extreme value theory. Extreme values are usually taken to follow either the generalized extreme value (GEV) distribution or the Poisson distribution in combination with the generalized Pareto distribution.

In this study, we have determined the probabilities of extreme sea levels and calculated return levels using the Revised Joint Probability Method (RJPM, Tawn and Vassie, 1989). A straightforward description of the method is given by Tsimplis and Blackman (1997), who used it in the Aegean Sea. The time series is separated into tide and tidal residual (hourly sea level minus tide). The tail of the distribution of the tidal residual maxima is estimated from the *r*-largest independent values of tidal residual per year by fitting the limit distribution of the *r*-largest order statistics (rGEV). The derived tidal residual distribution is then combined with the known tide distribution. In addition, the persistence of the extremes was accounted for through a parameter called the 'extremal index'. The application of RJPM requires the tide and the tidal residual to be independent, which is the case in low-tidal basins such as the Mediterranean (Marcos et al., 2009). For the Mediterranean Sea, the number of largest values of tidal residual per year (*r*) is commonly set to 5. This value has been found to be appropriate for the Mediterranean, as it allows for the inclusion of all major events but does not introduce nonextreme events (Tsimplis and Blackman, 1997; Marcos et al., 2009). In this study, we tested the method by changing *r* from 1 to 5 to quantify how it affects the return value estimates. To obtain reliable estimates using the rGEV method, individual events should be at least τ days apart to secure the independence of extreme values. In our study, we choose $\tau = 3$ d for positive extremes and $\tau = 6$ d for negative extremes. In the Mediterranean, τ is usually taken to be 3 d for positive extremes (Marcos et al., 2009). The average lifetime of midlatitude cyclones in the Mediterranean is 28 h (Trigo et al., 1999), strong (extreme producing) cyclones tend to move faster than weak cyclones (Lionello et al., 2019), and the use of an even shorter τ can be justified. However, upon surge relaxation, the Adriatic goes through a series of seiche oscillations before they damp out after ~3 d (Cerovečki et al., 1997), which introduces high autocorrelation within the sea level time series, and $\tau = 3$ d is thus needed to assure independence of the Adriatic positive extremes. Negative extremes are usually related to large-scale anticyclones that are present over the area for a longer time (Crisciani et al., 1994); therefore, we have chosen $\tau = 6$ d.

Confidence intervals were determined by the moving-block bootstrap (Lahiri, 2003). For both positive and negative extremes, we estimated the return values for several return periods: 2, 5, 10, 50 and 100 years.

2.3. Extraction of extreme episodes

Episodes of positive and negative extreme sea levels were extracted from the original series from which mean values were subtracted. Linear trends were not removed. An episode was defined as continuous interval of threshold-exceeding sea level. No criteria for a minimum time difference between two subsequent extreme episodes were imposed. This differs from the methodology used for the return levels analysis, for which independence of extreme values is a must, and for which a minimum threshold $\tau = 3$ (6) days was imposed for positive (negative) extremes (Section 2.2). While examining the data, we noticed that extreme episodes tend to cluster within groups, as will be detailed in subsequent sections. Successive extremes within a group are often dominated by different processes. The first positive extreme might, e.g., be due to an extreme storm surge, whereas the subsequent ones are likely to be influenced by tides (Međugorac et al., 2016) and seiche (Bajo et al., 2019). To estimate the contributions of different processes to the generation of Adriatic sea level extremes and to better evaluate the recently emphasized hazard of extremes repeating within a short interval (Thompson et al., 2019), we decided to extract and analyse all extreme episodes satisfying threshold criteria, regardless of their temporal distance. This approach mostly resulted in a minimum time difference between subsequent episodes of > 20 h. However, especially for the Highly Extreme Positive (HEP) episodes, at some stations, the two closest episodes were just 2–3 h apart.

Two types of positive extreme episodes were studied: (1) HEP episodes – episodes during which sea level surpassed the 99.99 percentile value measured at a station; (2) Extreme Positive (EP) episodes – episodes during which sea level surpassed the 99.95 percentile value measured at a station. Similarly, two types of negative extreme episodes were defined as well: (1) Highly Extreme Negative (HEN) episodes – episodes during which sea level was lower than the 0.01 percentile value measured at a station; (2) Extreme Negative (EN) episodes – episodes during which sea level was lower than the 0.05 percentile value measured at a station. Episodes defined by (2) include episodes defined by (1) for both positive and negative extremes. The duration of one episode was defined as the time during which sea level is above (below) the corresponding threshold, and the maximum (minimum) sea level height during a positive (negative) episode is taken to be the representative episode height. The percentile values and number of extracted events per station are given in Table 1.

Changes in the main features of the extreme episodes over ~65 years were examined through their linear trends. We estimated trends in the number of events per year, average duration per year and intensity. The intensity was defined as the largest threshold-exceeding sea level in each year. The trends with corresponding uncertainty intervals were determined using Bayesian statistics to account for autocorrelation within the time series. The autocorrelation was modelled as an AR(1) process. Details on the method can be found in Orlić et al. (2018). This approach allowed us to consider even episodes that occur within too short a time

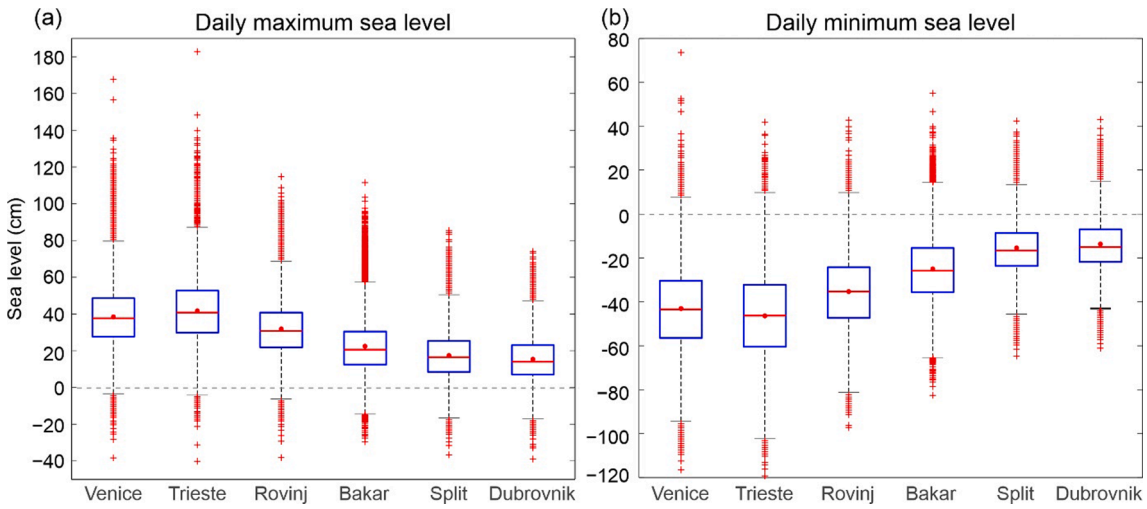

Fig. 2. (*a*) Distribution of daily maximum and (*b*) minimum hourly values of sea level over the 1956–2020 interval at Venice, Trieste, Rovinj, Bakar, Split, and Dubrovnik. Edges of the boxes (blue) represent the 25th and 75th percentiles, while the central line represents the median (red). Red circles represent mean value. Minima and maxima (excluding outliers) are indicated with highest and lowest marks (black). Outliers are marked with red crosses. (For interpretation of the references to colour in this figure legend, the reader is referred to the web version of this article.)

span for classical trend analysis to be justified. Whereas classical trend analysis would require more than a 3 d distance between EP and HEP and of > 6 d between EN and HEN, the Bayesian modelling framework can account for dependant extremes in a straightforward way. Furthermore, a restrictive classical approach would result in the removal of ~10–40% of the positive and ~25–85% of the negative extremes, as will be shown later. This could subsequently result in an underestimation of some processes that are likely to be more important for the extremes preceding and following the strongest one.

2.4. Decomposition of time series

We decomposed the sea level time series into seven components characterized by similar generation processes (detailed in the Introduction), spectral properties, and previously published methodologies (e.g., Pasarić et al., 2000; Vilibić and Šepić, 2010; Šepić et al., 2012b). These components are (1) *trend*; (2) *seasonal component*; (3) sea level oscillations at periods longer than 100 d (referred to as > 100 *d component* further in the text); (4) sea level oscillations at periods from 10 to 100 d (10–100 *d component*); (5) sea level oscillations at periods from 6 h to 10 days (6 *h*-10 *d component*); (6) *tide*; and (7) sea level oscillations at periods shorter than 6 h (< 6 *h component*). First, we determined linear trends using the least-squares method. Next, we estimated the seasonal signal by least-square fitting of the sum of the cosine functions of the annual and semiannual periods to the detrended time series:

$$f(t) = A_{365}cos\left(\frac{2\pi}{T_{365}}t + \varphi_{365}\right) + A_{182.5}cos\left(\frac{2\pi}{T_{182.5}}t + \varphi_{182.5}\right) \quad (1)$$

Periods of significant tidal peaks were then determined from spectra for each station. Depending on the station, between 37 and 43 tidal components were found to be significant ($p < 0.05$). The amplitudes and phases of each significant component were calculated using the least-squares method of tidal harmonic analysis, which was subsequently applied to year-long hourly sea level time series (Medvedev et al., 2020). It should be noted here that traditionally, only seven tidal components (diurnal: K_1, O_1 and P_1, and semidiurnal: M_2, S_2, N_2 and K_2) are estimated for the Adriatic Sea (e.g., Polli, 1959; Janeković and Kuzmić, 2005). However, Medvedev et al. (2020) showed that other tidal components are significant in the Adriatic as well and can contribute notably to tides. Means of the absolute differences between tides estimated using 37–43 components and tides estimated using only the 7 traditional components were found to be 3.77 cm for Venice, 3.93 cm for Trieste, 3.54 cm for Rovinj, 2.48 cm for Bakar, 2.11 cm for Split and 2.08 cm for Dubrovnik.

Residual time series were sequentially filtered using Kaiser-Bessel windows of lengths: 100 d, 10 d, and 6 h (e.g., Thomson and Emery, 2014). As a result of all listed procedures, the 7 components listed at the beginning of this chapter were obtained and analysed in detail.

Additionally, we estimated the contribution of the Adriatic fundamental seiche (~21.5 h) to HEP and EP episodes. The variability of sea level at the period of the seiche can be determined using a bandpass filter or wavelet method (Vilibić, 2006b). However, these approaches are not suitable if a previously generated seiche is to be distinguished from the newly induced seiche. Therefore, a semiempirical method proposed by Međugorac et al. (2015) was used to obtain an estimate of pre-existing seiche contributions to the observed maxima and minima. First, the 6 *h*-10 *d component* was visually inspected for the Adriatic fundamental seiche oscillations triggered up to 4 days before a peak of an EP (HEP) episode. If the seiche was indeed triggered, it was then modelled as a damped cosine with a period of 21.5 h and a decay time of 3.2 d (Cerovečki et al., 1997). Period was chosen as an average of values reported in the literature (e.g., Raicich et al., 1999; Lionello et al., 2005). An initial seiche amplitude at Trieste station was determined from the signal, considering sea level on periods shorter than 28 h. At other stations, the initial amplitude was estimated considering that the first mode decreases towards the open end of the Adriatic, using the spatial structure from Schwab and Rao (1983).

3. Return periods and climatology of the total Adriatic sea level extremes

3.1. Distributions and return periods

As the first step in the analysis of the Adriatic sea level extremes, we examined statistics of high and low waters based on time series of daily maximum and daily minimum levels (Fig. 2). The shown distributions reveal the main features of the Adriatic sea level extremes. The northern Adriatic (Venice, Trieste, Rovinj) experiences higher high levels and lower low levels than the middle/south Adriatic (Split, Dubrovnik), with the difference between median daily maxima (~40 cm in Trieste, ~15 cm in Dubrovnik) and minima (~-40 cm in Trieste, ~-15 cm in Dubrovnik) closely corresponding to the known spatial distribution of the mean tidal ranges over the Adriatic (Janeković and Kuzmić, 2005). Over the entire Adriatic, i.e., at each individual station, the heights of

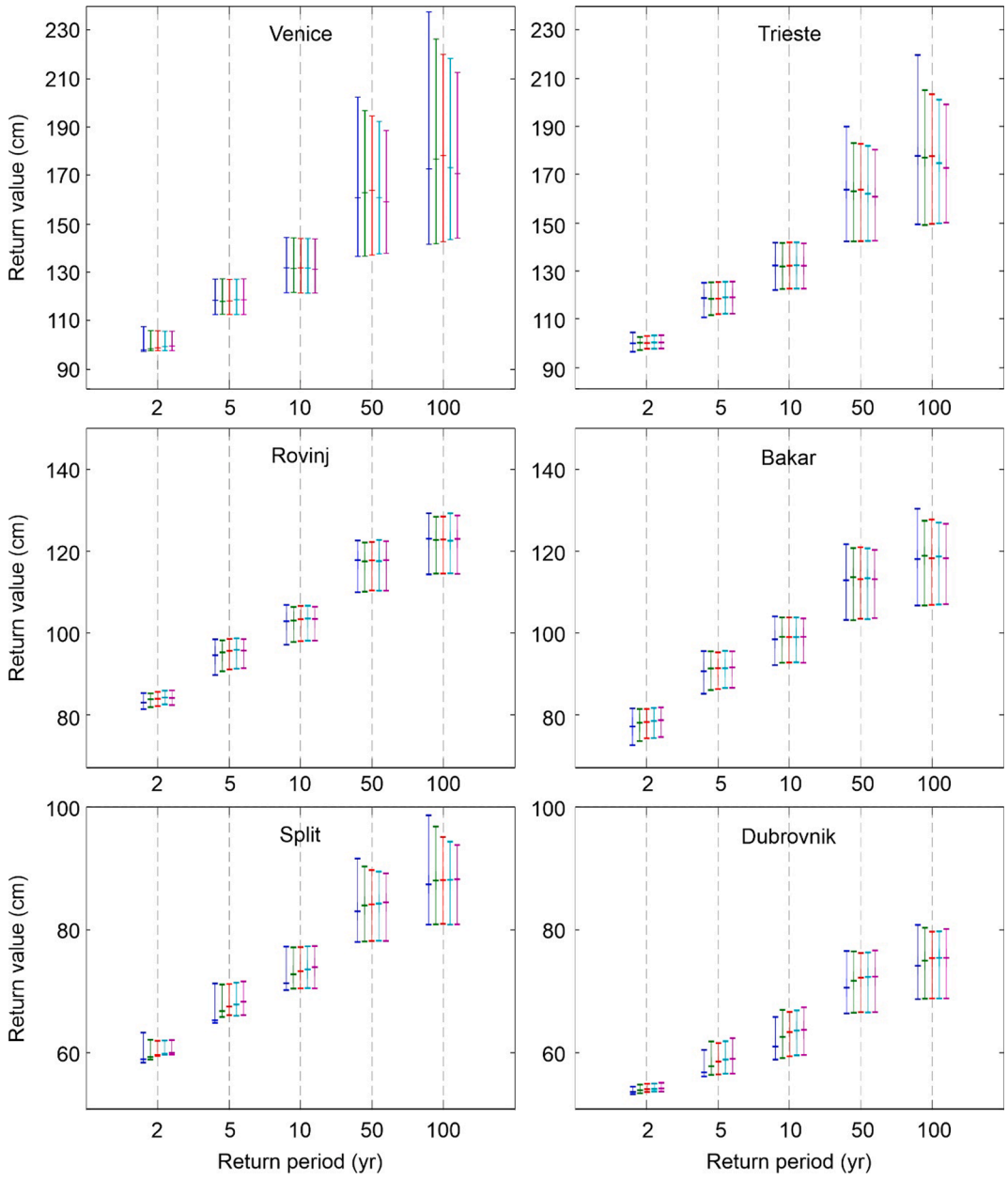

Fig. 3. Return values of maximum sea level for 2-, 5-, 10-, 50-, and 100-yr return periods with 95% confidence intervals, estimated by RJPM using $r = 1$ (blue) to 5 (magenta) largest tidal residuals per year. (For interpretation of the references to colour in this figure legend, the reader is referred to the web version of this article.)

the positive outliers (red crosses in Fig. 2a) are larger than the absolute heights of the negative outliers (Fig. 2b) by 15–25%. In contrast, the minima (lower black lines in boxplots; Fig. 2b) of the daily minimum values are larger (in absolute value) than the maxima (upper black lines in boxplots; Fig. 2a) of the daily maximum values for 10–20%, and the median and quartile values have comparable absolute values. Throughout the study, outliers are defined as those values that are greater than $q_3 + 1.5\times(q_3 - q_1)$ or lower than $q_1 - 1.5\times(q_3 - q_1)$, where q_1 and q_3 are the 25th and 75th percentiles of the sample data, respectively.

Return values of sea level maxima, obtained with $r = 1$ to 5 largest yearly values, for return periods of 2, 5, 10, 50 and 100 years are shown in Fig. 3. The dependence of return values on the choice of r is not uniform. In all cases, the difference is small (the largest is 7.5 cm at Venice for a 100-yr return period) and much smaller than the confidence interval, which is rather wide (for $r = 5$ up to 95.7 cm) in the northern Adriatic. The return values steadily decreases from the head of the basin (Trieste) to the southern Adriatic. The estimated 50-yr return level at Trieste is 160.7 cm ($r = 5$), almost the same as that at Venice (159.1 cm). In more southern parts of the northern Adriatic (Rovinj, Bakar), it is ~115 cm, and in the middle/south Adriatic, it is ~70–85 cm. These values roughly agree with the ones plotted in Marcos et al. (2009), although their time series stop earlier, and with the return values estimated by Masina and Lamberti (2013) (their analysis is done using only November extreme events). Somewhat different return values were obtained for Venice and Trieste by Pirazzoli et al. (2007), but they did not use a time threshold τ for separating successive extreme events. It should be noted that our estimated return periods (especially when considering events distanced for > 10–20 years from present) do not take into account future changes in mean sea level or possible changes in ocean, atmospheric, hydrological and geological processes that govern sea level extremes.

Absolute return values for negative extremes (Fig. 4) are smaller than return values for positive extremes, as anticipated from Fig. 2, especially

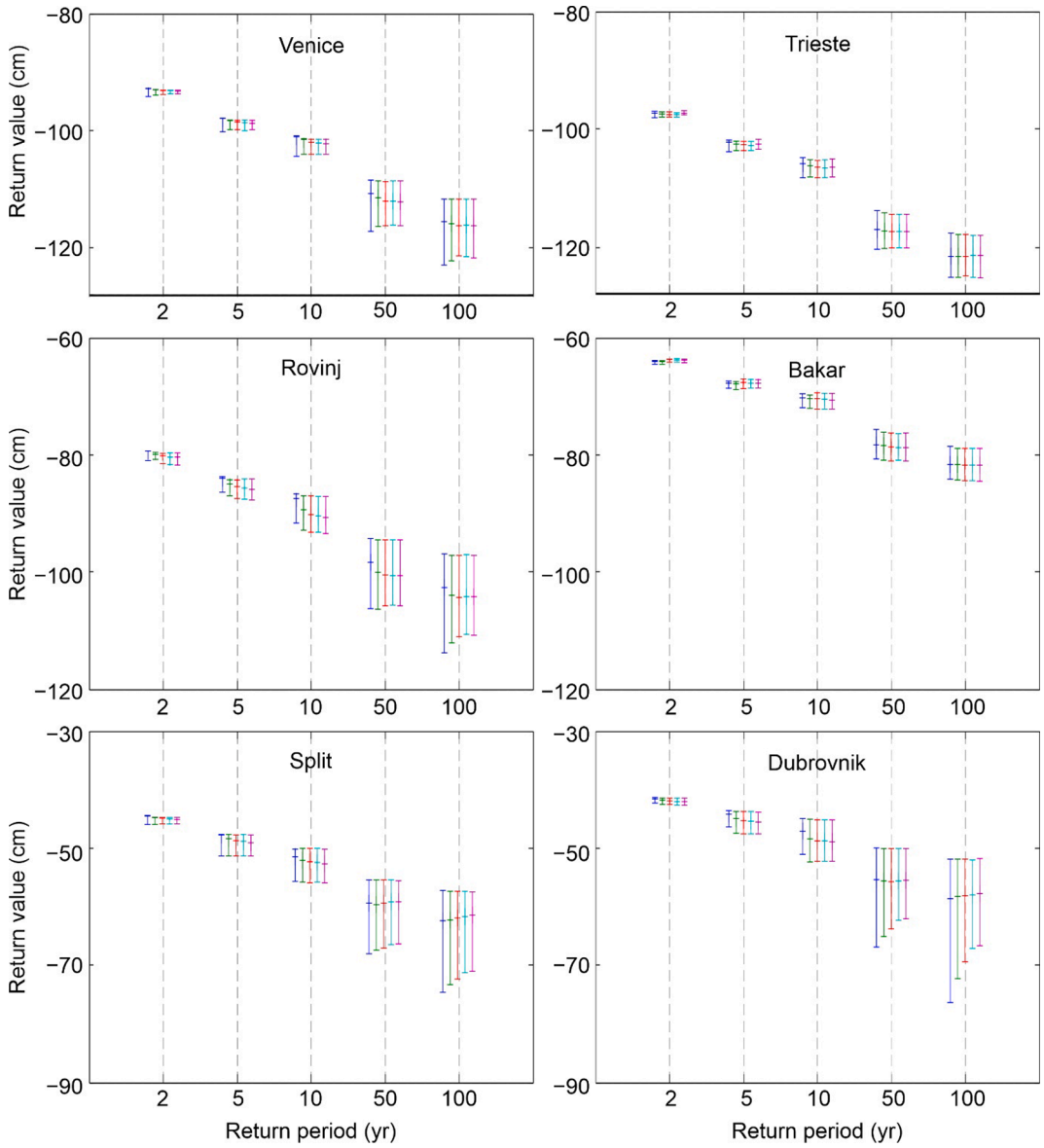

Fig. 4. Return values of minimum sea level for 2-, 5-, 10-, 50-, and 100-yr return periods with 95% confidence intervals, estimated by RJPM using $r = 1$ (blue) to 5 (magenta) lowest tidal residuals per year. (For interpretation of the references to colour in this figure legend, the reader is referred to the web version of this article.)

for longer return periods. The estimated values do not change much with *r,* but the confidence intervals decrease when more than one extreme per year is considered. The lowest return values, similar to the highest values, are estimated for the northernmost Adriatic – the 50-yr level at Trieste and Venice is ∼-115 cm, and they steadily increase towards the south - so, at Dubrovnik, the 50-yr return value is half of that at the northern Adriatic (-55 cm). The confidence intervals for the negative extremes are much narrower in the north than farther south, as opposed to the ones estimated for the positive extremes.

3.2. General characteristics of the extreme events

We now move to the analysis of the extreme episodes extracted according to the procedure described in Section 2.3. The 0.01, 0.05, 99.95 and 99.99 percentile values of sea levels estimated for each station are given in Table 1, along with the total number of extracted events and average number of events per year. The values of observed maxima and minima, as well as absolute values of positive and negative percentiles, gradually increase towards the north, with absolute values for Dubrovnik smaller by ∼50% than absolute values for Venice and Trieste. The number of extreme episodes also increases from the south to the north for all types of episodes, aside from HEP (Table 1). It can be further noticed that the number of negative episodes is slightly larger than the number of positive episodes, pointing to a moderately different distribution of positive and negative extremes at all stations, as discussed previously (Fig. 2 and Fig. 3).

An example of a time series with the indicated EP and EN episodes is given in Fig. 5. Strengthening of extremes towards the north is evident herein as well: sea levels reached > 100 cm in Trieste and Venice and $<$ 60 cm in Split and Dubrovnik during the two marked EP episodes; similarly, during several EN episodes, the sea dropped to levels below −100 cm in Trieste and Venice and just slightly below −50 cm in Split and Dubrovnik. All marked EP episodes occurred during prolonged periods of increased background sea levels (sea level higher than its mean value for at least 20 d), and all marked EN episodes occurred during prolonged periods of lowered background sea levels (sea level lower than its mean value for at least 15 d). Both the highest and lowest sea levels were reached when shorter period processes were superimposed onto the background sea level. A certain spatial synchronicity of positive and negative episodes can also be noticed. During the pictured periods,

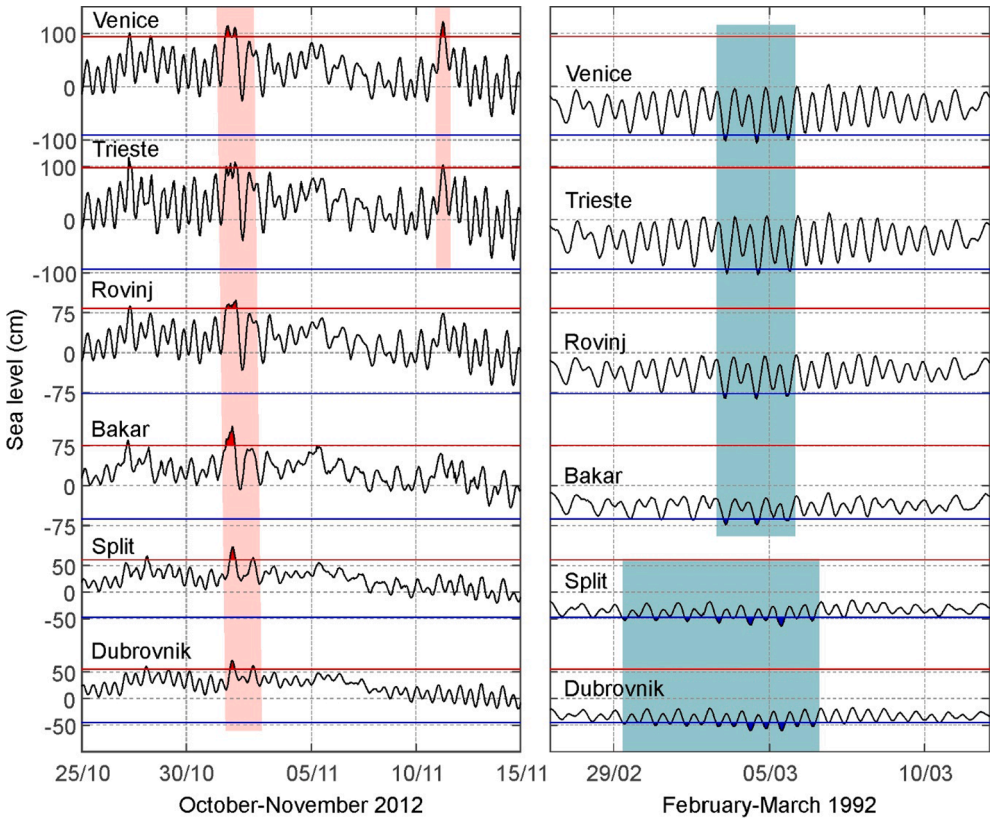

Fig. 5. Example of time series with positive (*left*) and negative (*right*) sea level extremes; 99.95 and 0.05 percentiles are marked by red and blue lines, respectively. Intervals surrounding the EP episodes are shaded in light red, and intervals surrounding the EN episodes are shaded in light blue. (For interpretation of the references to colour in this figure legend, the reader is referred to the web version of this article.)

one EP and several EN episodes occurred almost simultaneously at all stations, whereas one EP episode was recorded at the Venice and Trieste stations only, and a couple of EN episodes clustered within a group at the Split and Dubrovnik stations only.

The number of positive and negative episodes per year is shown in Fig. 6. Instantly, we notice what seems to be a positive trend of EP and HEP episodes and a negative trend of EN and HEN episodes. However, there are only three significant trends: a negative trend in the number of EN episodes in Trieste and positive trends in the number of EP episodes in Venice and Dubrovnik (Table 2). A strong decadal variability in the number of extreme episodes stands out (Fig. 6). The highest number of positive extremes was recorded during 2009–2014, with as many as 19 EP episodes recorded in Dubrovnik in 2010 (15, 8, 8, 8 and 6 in Split, Bakar, Rovinj, Trieste and Venice, respectively), followed by the 2018–2020 period. Throughout the remaining period, variability in the number of positive episodes was less pronounced, especially over the northern Adriatic (Venice, Trieste, Rovinj and Bakar). However, over the middle (Split) and southern (Dubrovnik) Adriatic, two periods during which almost no positive events were recorded stand out: the first of these periods spans most of the 1970s, and the other period covers the years from the early 1980s to the mid-1990s. During both these periods, positive extremes were still present over the northern Adriatic. The numbers of negative episodes show almost opposite distributions. Two periods with an increased number of extreme negative events can be noticed: one centred approximately in 1990, when a consistent number of EN episodes (~10 per year) was observed at all stations, and the other centred approximately in 1959, when numerous negative episodes were recorded at the Dubrovnik (19), Split (10), Rovinj (14), Venice (10) and Trieste (9) tide gauges. Most of the 1959 events were observed in February. No sea level measurements were available for Bakar for February 1959; therefore, no events were recorded there. Conclusively, we can say that the decadal variability of both positive and negative extremes in the Adriatic Sea was more important than an underlying trend in their numbers. The decadal variability of extremes has been previously noticed (Stravisi and Ferraro, 1986; Unal and Ghil, 1995; Orlić and Pasarić, 1994, 2000).

3.3. Seasonal distribution of the total extremes

The seasonal distribution of positive and negative episodes is shown in Fig. 7. Over the northern Adriatic, EP episodes dominantly occur during November and December (58–68% of events, depending on station). Going to the more extreme events, the seasonal distribution is even more evident: 61–81% of all northern Adriatic HEP episodes occurred during November and December. Noticeable numbers of EP episodes and a few HEP episodes were also recorded during October, January, February, and March at the four northern Adriatic stations, whereas almost no EP and HEP episodes were recorded from April to September. Further to the south (Split and Dubrovnik), EP and HEP episodes were relatively uniformly distributed through November, December and January, with a total of 77–81% of EP and 80–82% of HEP episodes occurring within these three months, depending on the station. The negative extremes also showed a pronounced seasonal distribution. Over the northern Adriatic, most EN and HEN events were recorded in January and February (71–84% for EN, 72–90% for HEN), with a much lower number of episodes observed during November and March and just a few episodes during June to August. In the middle and southern Adriatic, almost all recorded EN and HEN episodes occurred during late winter, i.e., from February to March (94–100%). Conclusively, there was a strong seasonal distribution of positive and negative extremes in the Adriatic Sea, with a slightly different distribution of months with the highest number of events between the northern and the middle and southern Adriatic.

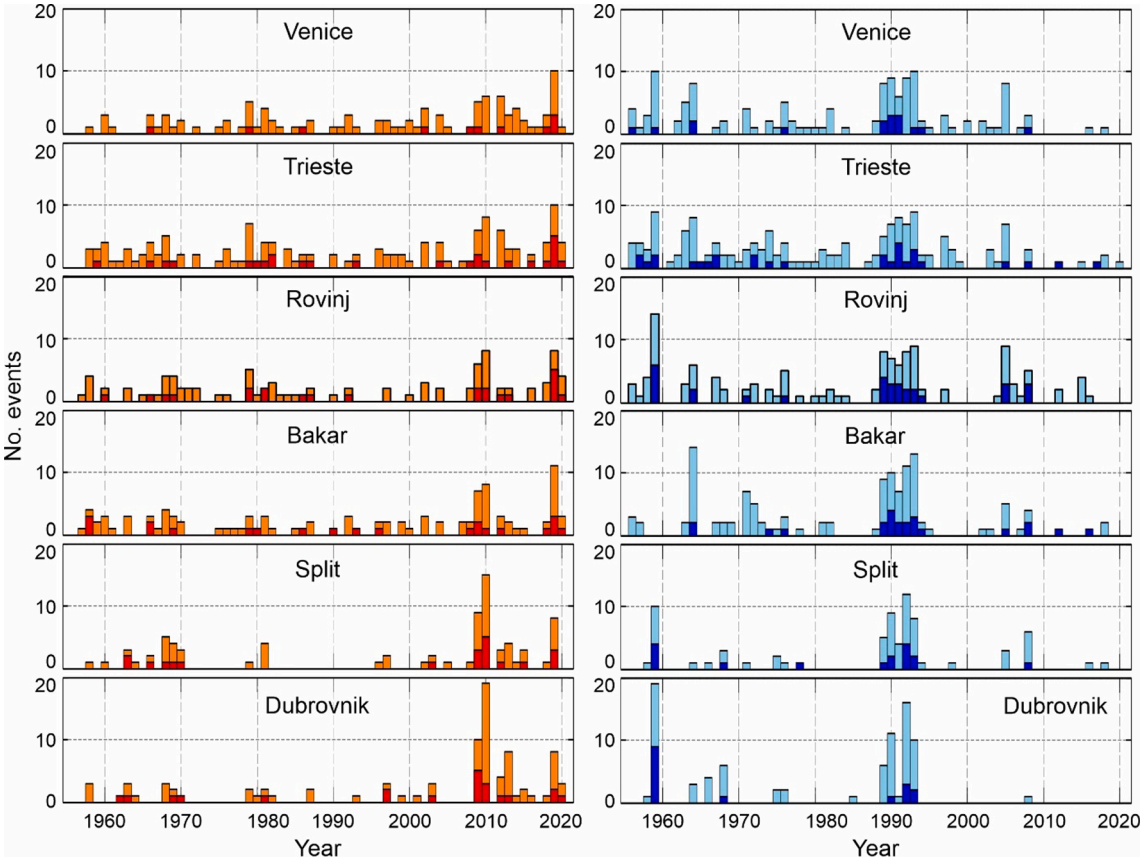

Fig. 6. Number of positive extreme events (*left*) and negative extreme events (*right*) per station per year. Orange columns represent EP, red represents HEP, light blue represents EN, and dark blue represents HEN episodes. (For interpretation of the references to colour in this figure legend, the reader is referred to the web version of this article.)

3.4. Duration of the total extremes

The duration of positive and negative extremes is presented in Fig. 8. The average duration is generally short – EP episodes last on average 2 h at the northern Adriatic stations and 3 h at the middle and southern Adriatic stations, whereas HEP episodes last on average 2 h at all stations. For the negative extremes, EN episodes, on average, lasted 2 h in the northern Adriatic and 3 h in the middle and southern Adriatic. Naturally, HEN episodes are slightly shorter, i.e., they last between 1 and 2 h in the northern Adriatic and 3 h in Split and Dubrovnik. We can conclude that the mean durations of positive and negative extremes are comparable. However, distributions of durations are somewhat different: in general, the 75th percentile of duration of positive extremes was higher than the 75th percentile of duration of negative extremes over the northern Adriatic, and there are many more outliers related to EP episodes than to EN episodes. This was particularly true for the northern Adriatic stations, where a couple of EP episodes with durations longer than 10 h were recorded. These were the well-researched 1966 and 2012 northern Adriatic floods. The 1966 episode was the most disastrous flood ever recorded in Venice, and it occurred because of a storm surge induced by uniform sirocco continuously blowing for more than a day (Međugorac et al., 2015). Canestrelli et al. (2001) reported that on this occasion, water in Venice stayed over 110 cm (in reference to the local zero) for 22 h, flooding a greater part of the city. However, the 2012 event was an outcome of storm surge and tide superimposed on a prolonged interval of raised water due to the larger-scale process (Međugorac et al., 2016). Adriatic tide gauges, especially those on the northeastern side, recorded exceptional water levels on this occasion, with hourly sea levels in Bakar rising to the highest level ever observed.

Trends of durations of extreme episodes reveal shortening of negative and lengthening of positive episodes (Table 2), with significant trends related to shortening of EN episodes in Venice, Trieste, Split and Dubrovnik – from −0.67 h/10 year (Split) up to −2.00 h/10 year (Venice); and to lengthening of EP episodes at all stations but Split – from 0.52 h/10 year (Trieste) up to 2.77 h/10 year (Venice).

3.5. Intensity of the total extremes

Finally, we examined trends related to the intensity of the extreme episodes (Table 2). A significant increase in the intensity of HEP episodes, ranging from 0.89 cm/10 year (Bakar) to 3.23 cm/10 year (Venice), was obtained for all stations, aside from Trieste, for which a significant decrease in intensity was obtained. EP episodes show the opposite trend and decrease in intensity, with significant trends estimated for Venice and Trieste. Trends of intensity of EN and HEN episodes were mostly not significant and of varying sign, depending on station and episode type.

4. Analysis of the sea level components

4.1. Spectral analysis

The spectra of the analysed sea level time series are given in Fig. 9. The cut-off periods, selected for decomposition of series, are indicated as well. The spectra can be visually separated into three different parts: the first, which covers periods longer than approximately 30–40 days and for which the slope of the spectra is relatively mild; the second, which covers periods from approximately 6 h to 30–40 d and at which spectral energies decay with the ω^{-2} law (Kulikov et al., 1983); and the third, which encompasses periods shorter than 6 h at which the spectral slope

Table 2
Trend (i.e., change in 10 years) of a) number, b) duration and c) intensity of sea level EP, HEP, EN and HEN episodes, with 95% credible intervals in brackets. Nonzero trends are given in bold.

(a) **Number of events (1/10 years)**

Type	Venice	Trieste	Rovinj	Bakar	Split	Dubrovnik
HEN	−0.35 [-1.20, 0.64]	−0.08 [-0.22, 0.07]	−0.03 [-0.24, 0.18]	0.02 [-0.26, 0.30]	−0.06 [-0.29, 0.17]	−0.13 [-0.31, 0.06]
EN	−1.02 [-2.26, 0.27]	**−0.46** [-0.90, −0.02]	−0.25 [-0.74, 0.23]	−0.23 [-0.78, 0.32]	−0.10 [-0.64, 0.45]	−0.32 [-0.76, 0.12]
EP	**0.89** [0.30, 1.45]	0.21 [-0.10, 0.53]	0.17 [-0.16, 0.53]	0.21 [-0.14, 0.56]	0.16 [-0.23, 0.55]	**0.49** [0.03, 0.95]
HEP	0.31 [-0.08, 0.67]	0.08 [-0.06, 0.22]	0.09 [-0.03, 0.21]	0.01 [-0.11, 0.14]	0.00 [-0.09, 0.10]	0.10 [-0.06, 0.26]

(b) **Duration (h/10 years)**

Type	Venice	Trieste	Rovinj	Bakar	Split	Dubrovnik
HEN	−0.64 [-1.88, 0.71]	−0.04 [-0.27, 0.19]	−0.05 [-0.38, 0.30]	0.04 [-0.56, 0.63]	−0.21 [-0.63, 0.21]	**−0.39** [-0.77, −0.01]
EN	**−2.00** [-3.19, −0.79]	**−0.83** [-1.28, −0.38]	−0.41 [-0.87, 0.05]	−0.32 [-0.84, 0.19]	**−0.67** [-1.12, −0.22]	**−1.36** [-1.76, −0.96]
EP	**2.77** [1.87, 3.67]	**0.52** [0.08, 0.95]	**0.74** [0.28, 1.21]	**0.58** [0.16, 0.99]	0.35 [-0.06, 0.76]	**1.51** [1.06, 1.95]
HEP	0.59 [-0.30, 1.41]	0.17 [-0.12, 0.46]	0.34 [-0.01, 0.71]	0.15 [-0.15, 0.46]	0.15 [-0.14, 0.43]	0.32 [-0.10, 0.73]

(c) **Intensity (cm/10 years)**

Type	Venice	Trieste	Rovinj	Bakar	Split	Dubrovnik
HEN	1.06 [-1.38, 3.58]	−0.12 [-0.71, 0.47]	−0.50 [-1.45, 0.44]	−0.06 [-0.53, 0.42]	0.25 [-0.01, 0.51]	0.03 [-0.61, 0.69]
EN	**2.03** [0.35, 3.68]	−0.21 [-0.68, 0.25]	0.02 [-0.68, 0.71]	0.03 [-0.63, 0.69]	0.13 [-0.34, 0.65]	−0.18 [-0.89, 0.58]
EP	**−1.59** [-2.64, −0.54]	**−0.93** [-1.36, −0.51]	−0.52 [-1.06, 0.03]	−0.17 [-0.62, 0.29]	−0.25 [-0.83, 0.33]	−0.25 [-0.77, 0.25]
HEP	**3.23** [1.43, 5.06]	**−1.58** [-2.10, −1.05]	**1.50** [0.76, 2.24]	**0.89** [0.27, 1.48]	**1.13** [0.58, 1.72]	**0.95** [0.12, 1.72]

becomes milder at some stations again. At low frequencies, two small, but significant, spectral peaks stand out – these were evident at all stations and are related to the seasonal signal, i.e., to the sea level oscillations occurring at the semiannual (182.5 d) and annual (365 d) periods. These peaks correspond to the *seasonal component*. A series of pronounced spectrum peaks can be noticed at diurnal, semidiurnal and shorter periods - these narrow and high peaks are related to *tides*. Three broad peaks centred at approximately 21.2, 12.4–10.9 and 6.7 h correspond to the fundamental (21.2 h), first (10.9 h) and second (6.7) modes of the Adriatic seiche (Schwab and Rao, 1983; Cerovečki et al., 1997; Raicich et al., 1999; Pasarić and Orlić, 2001) and other eigen oscillations. The spectra of all stations are relatively similar up to periods of 6 h, with the differences between stations emerging at shorter periods. In the Trieste spectrum, there are wide peaks centred at 3.8 and 5.3 h. The 3.8 h peak can be attributed to the Trieste Bay seiche, which has a period of 2.7–4.2 h (Caloi, 1938; Cushmain-Roisin et al., 2001; Šepić et al., 2012a), and origin of the 5.3 h peak is unclear. In the Bakar spectrum, there is increased energy at periods centred at 2.0 and 3.2 h, of which the first corresponds to the first mode of Kvarner Bay seiches (Goldberg and Kemplni, 1938; also previously reported bySepić et al., 2008) and the latter has not been reported previously in the literature. For the Split spectrum, the observed peaks centred at 4.1 h and 2.6 h correspond to the fundamental and first modes of the wider local area seiche (Vilibić et al., 2005; Šepić et al., 2016).

4.2. General characteristics of the sea level components

An example of sea level time series decomposition for stations Trieste, Bakar and Dubrovnik is shown in Fig. 10. Immediately, it can be noticed that there are components that are rather uniform over the Adriatic (both in terms of phase and amplitude) and that there are components that strongly differ between the middle/southern and the northern Adriatic. The latter are the 6 *h*-10 *d component*, *tide* and < 6 *h component*.

Trends of mean sea level ranged from 0.99 mm/yr in Rovinj to 2.26 mm/yr in Venice, which are values comparable to those listed in the Introduction. At periods longer than 100 d, the Adriatic Sea behaves uniformly – oscillations are in phase, and their amplitudes differ only slightly (Fig. 10a, Fig. 11). The most pronounced characteristic of the $>$ 100 *d component* was a strong decadal variability with two intervals standing out: (1) period of extremely low sea levels during several years centred around the year 1990 (dropping to −20 cm at most stations); and (2) period of increased sea levels during several years centred around the year 2010 (sea level up to 20 cm at most stations). These two periods correspond, respectively, to the (1) period characterized by a larger-than-usual number of negative extremes (Fig. 6 *right*) and to (2) the period characterized by a larger-than-usual number of positive extremes (Fig. 6 *left*). This matching of periods implied that the $>$ 100 *d component* preconditions the yearly rate of occurrence of extreme events.

Next comes the *seasonal component* – similar to the $>$ 100 *d component*, seasonal oscillations are in phase over the entire Adriatic (Fig. 10b), and they are of comparable amplitude (Fig. 10b, Fig. 11). However, the range of the *seasonal component* has a weak south to north gradient: in Dubrovnik, the difference between the 99.99 and 0.01 percentiles equals ~10 cm, whereas over the northern Adriatic, this difference reaches ~15 cm in Venice and ~14 cm in Trieste (Fig. 11). For the 10–100 *d component*, sea level oscillations are again comparable over the northern and middle/southern Adriatic, especially when phases are considered (Fig. 10b). In regard to amplitudes, the absolute values of extreme percentiles (99.95, 99.99, 0.05 and 0.01) slightly increases towards the north, remaining within a 10 cm limit.

The 6 *h*-10 *d component* and *tide* are characterized by pronounced south-to-north differences (Fig. 10c, Fig. 11). The corresponding amplitudes are up to 3 times larger over the shallow northern than over the deeper middle/southern Adriatic, and the phases and shapes of the time series differ as well. In Trieste, where the tidal oscillations are the strongest, the 99.95 percentile value of *tide* reaches 60.2 cm, and the 99.99 percentile value reaches 62.6 cm. In Dubrovnik, the corresponding values are 23.7 cm for the 99.95 percentile and 24.4 cm for the 99.99 percentile. The same conclusion is reached when 0.05 and 0.01 percentile values are considered; in Trieste, these reach −71.8 and −74.6 cm, and in Dubrovnik −19.9 and −20.6 cm, respectively. There is also a phase shift between the southern and the northern Adriatic *tide* (not immediately discernible in Fig. 10c) – the shift occurs since semidiurnal tidal components propagate as Kelvin and Poincaré waves in the Adriatic (Hendershott and Speranza, 1971; Medvedev et al., 2020), accounting for the phase difference of the main components of 167° between Dubrovnik and Trieste (Medvedev et al., 2020).

An inspection of the 6 *h*-10 *d component* reveals a similar south-to-north gradient; over the northern Adriatic, the 99.95 and 99.99 percentile values are highest in Venice, reaching 51.9 and 67.9 cm, respectively. Over the southern Adriatic, in Dubrovnik, the corresponding values are 21.9 and 27.9 cm. The absolute values of the 0.05 and 0.01 percentiles of the 6 *h*-10 *d component* are much smaller, and the south-to-north gradient is somewhat less pronounced, ranging from −16.0 (-19.9) cm in Dubrovnik to –33.7 (-42.3) cm in Trieste for the 0.05 (0.01) percentile. Out of all components considered thus far, the 6 *h*-10

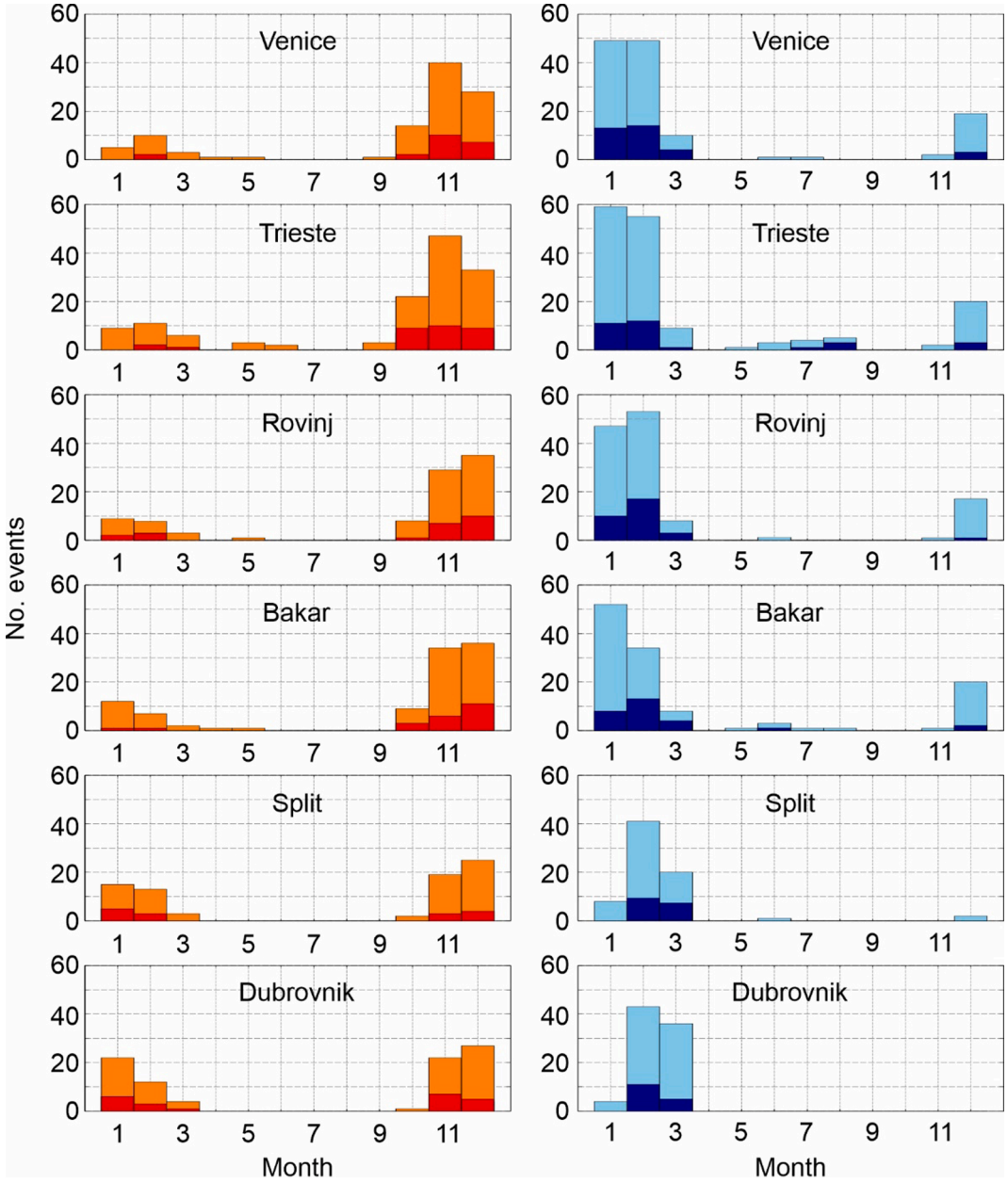

Fig. 7. Seasonal distribution of sea level extremes: number of positive (*left*) and negative (*right*) extreme episodes per station per month. Orange columns represent EP, red represents HEP, light blue represents EN, and dark blue represents HEN episodes. (For interpretation of the references to colour in this figure legend, the reader is referred to the web version of this article.)

d component changes the most over the Adriatic Sea (Fig. 10c); however, maxima and minima of the 6 *h*-10 *d component* over different parts of the Adriatic seem to be reached within several day spans, implying a certain simultaneity of the underlying processes (Fig. 10c; and Section 5.3).

Ending with the shortest period, the < 6 *h component* is characterized by the lowest oscillation ranges (Fig. 10d, Fig. 11). No pronounced south-to-north gradient is evident. Oscillations are strongest at Trieste, where 99.95 (99.99) percentile values reach 12.7 (18.4) cm, and 0.05 (0.01) percentile values reach −12.3 (-18.4) cm. The weakest oscillations were recorded in Dubrovnik. The symmetry between positive and negative extremes is to be expected, as these high-frequency oscillations are normally related to seiches that have similar positive and negative amplitudes (Rabinovich, 2009). In addition, oscillations of the < 6 *h component* are known to appear over spatially limited sections of the coast as they are generated by mesoscale atmospheric features of O (10–100 km) dimensions (e.g., atmospheric gravity waves, convective jumps, etc.; Rabinovich, 2020). Due to this, there were numerous situations when pronounced < 6 *h component* sea level oscillations were recorded only at one station (e.g., two episodes during July 1995 recorded only in Trieste, or one episode during late October 1995 recorded only in Dubrovnik, Fig. 10d). Occasionally, however, oscillations at periods shorter than 6 h appear over the entire Adriatic within 1–2 days. An example is given in Fig. 12, in which we showed a high-frequency event of 28–29 August 1995. During this time, the high-frequency oscillations first started at Trieste, then half a day later at Bakar, and additional several hours later, a single jump in sea levels was recorded at Dubrovnik.

The seasonal distribution of extremes of individual sea level components mostly follows the seasonal distribution of total extremes (Fig. 7), with most components reaching the following: (1) their maxima values in November and December, i.e., during months when EP and HEP episodes prevail; (2) their minima values from January to March, i.

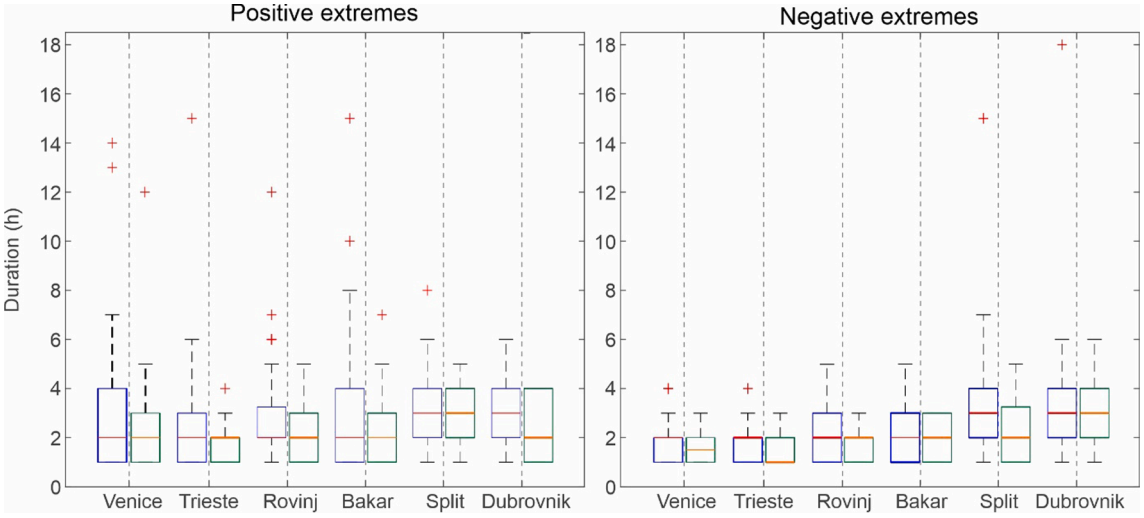

Fig. 8. Boxplots of the duration of positive (*left*) and negative (*right*) extremes; blue-red boxplots represent EP and EN episodes, and green-orange boxplots represent HEP and HEN episodes. The edges of the boxes represent the 25th and 75th percentiles, while the central line represents the median. Minima and maxima (excluding outliers) are indicated with highest and lowest marks (black). Outliers are marked with crosses. (For interpretation of the references to colour in this figure legend, the reader is referred to the web version of this article.)

e., during months when EN and HEN episodes prevail. Detailed analysis is given in Appendix A. In Appendix B, we show that the duration of extremes is dominantly governed by the duration of extreme values of *tide* and 6 *h*-10 *d components*.

5. Contribution of components to extreme events

Box plots showing the percentage of component contributions to positive (Fig. 13a) and negative (Fig. 13b) extremes are shown. Significant differences exist between (1) the positive and negative extremes and (2) the northern and the middle/southern Adriatic.

5.1. Positive extremes

Over the northern Adriatic (Venice, Trieste and Rovinj), the components that contribute the most to the positive extremes are the 6 *h*-10 *d component* and *tide*. If we look at the median values, the two jointly contribute ~70% to both EP and HEP episodes. For EP episodes, the average contribution of *tide* is more important than the contribution of the 6 *h*-10 *d component*, whereas the opposite is true for HEP episodes. The outlier values were such that they increase the relative contribution of the 6 *h*-10 *d component* (up to 80.3% in Trieste) and decrease the relative contribution of *tide* (down to –22.9% in Trieste), implying that the governing atmospheric processes (cyclones and sirocco winds), which are manifested in the 6 *h*-10 *d component* sea level oscillations, can be of such strength and importance that they overcome even the negative phase of the tidal signal. Such was the case during the record-breaking 4 November 1966 Venice flood, when the contribution of *tide* was negative (Međugorac et al., 2015). Going slightly to the south, to Bakar, we notice that the 6 *h*-10 *d component* becomes more important than *tide* for both EP and HEP episodes and that the relative contribution of the 10–100 *d component* increases. This agrees well with the estimated 99.95 and 99.99 percentile component values for Bakar (Fig. 11). Over the middle (Split) and southern (Dubrovnik) Adriatic, three components (10–100 *d*, 6 *h*–10 *d*, and *tide*) contribute evenly to the total positive extremes, with respective medians explaining ~75% of EP and 71.8–78.1% of HEP episodes at both stations.

The contribution of the *trend* to extremes was mostly approximately zero or weakly positive (up to 5.3% for HEP in Dubrovnik), indicating that a similar number of EP and HEP episodes occurred during the first and second halves of the time series (also confirmed by mostly nonsignificant trends; Table 2). The contribution of the $>$ 100 *d* component increases from north to south, spanning median contributions ranging from 6.8% (Trieste) to 15.0% (Split) for EP episodes and from 5.5% (Venice) to 16.1% (Split) for HEP episodes.

At all stations, the contribution of the *seasonal component* to the positive extremes is relatively small (Fig. 13a), with a median value between 3.9% in Trieste and 6.4% in Dubrovnik. However, the contributions of *seasonal components* are almost always positive, indicating that sea level extremes occur dominantly during the seasonal signal maximum, i.e., between October and December. The contribution of the seasonally elevated sea level to the overall extremes is slightly larger in the southern Adriatic (25 and 75 percentile values at Dubrovnik of EP episodes are 4 and 11%, respectively) than in the northern Adriatic (25 and 75 percentile values of EP episodes at Trieste are 1 and 6%, respectively), in contrast to the range of seasonal signals, which is larger over the northern than over the middle/southern Adriatic.

As opposed to other components, the contribution of the $<$ 6 *h component* does not change uniformly from the north towards the south. The contribution was most significant in Trieste during the studied period. Although the median contribution was not high, only 4.3% for the EP episodes, there were 8 outlier EP episodes during which the $<$ 6 *h component* contributed to the total heights of up to 33.1%. This component can also be important in Bakar (contributing up to 16.1% to EP episodes), whereas at other stations, its contribution does not surpass 10.0%, even when outliers are considered. The amplitude of the $<$ 6 *h component* is related to the local bathymetry features: at those stations that are located in the bays, i.e., at which seiche activity is usually strong (e.g., Trieste, Bakar), the contribution of the $<$ 6 *h component* is expectedly much more important than at those stations that are located on the open coast (e.g., Dubrovnik station).

We have also estimated the contribution of a fundamental mode of a pre-existing Adriatic-wide seiche to the positive extremes (Fig. 14, Fig. 15). The period at which the seiche occurs is ~21.2 h (Cerovečki et al., 1997), and thus, it is contained within the 6 *h*-10 *d component*. Seiches can positively or negatively contribute to the Adriatic floods (Fig. 14). Comparing contributions at different stations, the highest values are achieved at Rovinj, where the Adriatic seiche can reach 49% of the total and even 97% of the 6 *h*-10 *d* sea level, closely followed by Bakar and Trieste, and to a lesser extent Venice (Fig. 14). Fig. 11 and Fig. 13a indicate that extremes of the 6 *h*-10 *d component* in Rovinj are lower than would be expected based on values from the surrounding stations. This is a result of the spatial distribution of storm surges, which have a local minimum over the western Istria (Rovinj) coast (Međugorac

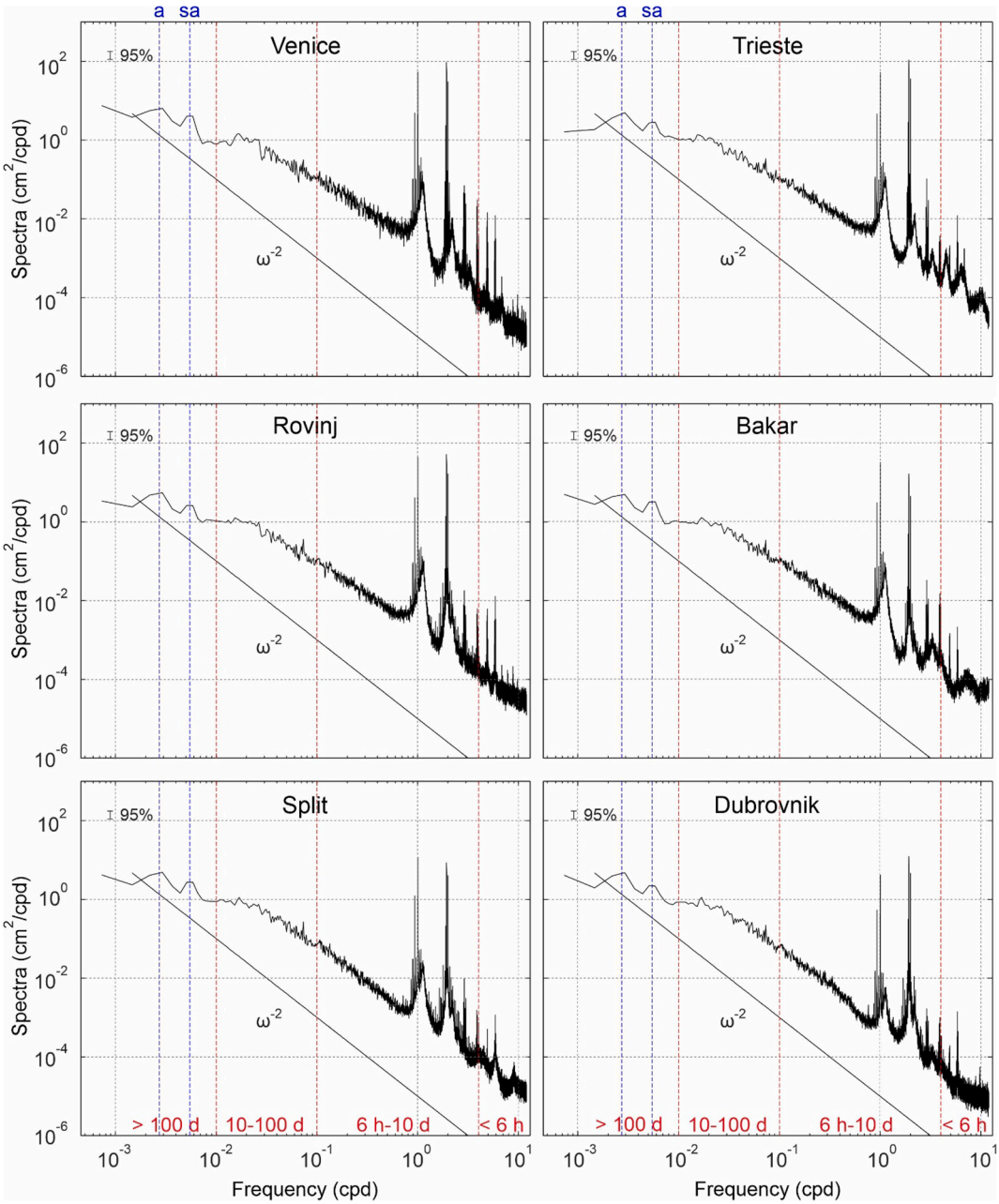

Fig. 9. Spectra of sea level time series measured at Venice, Trieste, Rovinj, Bakar, Split, and Dubrovnik. Cut-off frequencies are indicated with dashed red lines, frequencies of the annual and semiannual signals with dashed blue lines, ω^{-2} curve with black line. The confidence interval (95%) is given in the upper left corner of each plot. (For interpretation of the references to colour in this figure legend, the reader is referred to the web version of this article.)

et al., 2018), and the Adriatic-wide seiche, which does not have such a minimum (Schwab and Rao, 1983); thus, the seiche-to-synoptic (6 *h*-10 *d*) ratio is highest in Rovinj. The percent contribution of the pre-existing seiche decreases towards the south (Fig. 14), likely because the seiche amplitudes diminish much faster towards the south than the amplitude of the 6 *h*-10 *d component*. The seiche amplitude in Dubrovnik is ~15% of the seiche amplitude in the northern Adriatic (Schwab and Rao, 1983), whereas according to our analysis, extreme values associated with the 6 *h*-10 *d component* in Dubrovnik are ~40–45% of the corresponding extreme values of the 6 *h*-10 *d component* over the northern Adriatic (Fig. 11). As an example, Fig. 15 shows the evolution of the seiche excited prior to the three chosen EP episodes (18 December 1958 and two episodes on 24 and 25 December 2009). The 1958 event was an EP episode at stations Bakar and Rovinj – it was preceded by another EP episode (17 December), which gave onset to an extremely strong seiche – the seiche contributed to the episode of 18 December with 12 cm in Bakar and 12 cm in Rovinj. During 23–25 December 2009, three EP episodes were recorded at the northern Adriatic stations. The first episode (23 December) strengthened the already active Adriatic seiche, which subsequently generated almost the entire maxima of the 6 *h*-10 *d* component of the 24 December EP episode, which then also contributed (but to a lesser extent) to the height of the third, 25 December EP episode. Evidently, our method does not reproduce complete seiche activity, but it gives an order of magnitude of seiche contribution to an upcoming storm surge. In this way, the main features of a previously generated seiche were modelled, and its effect, positive or negative, on an upcoming flood was estimated. It should be emphasized that the method assumes a unique period (21.5 h) and a unique decay time (3.2 days), which may not be valid for all seiche cases, particularly those influenced by cross-basin winds (Cerovečki et al., 1997). Generation of

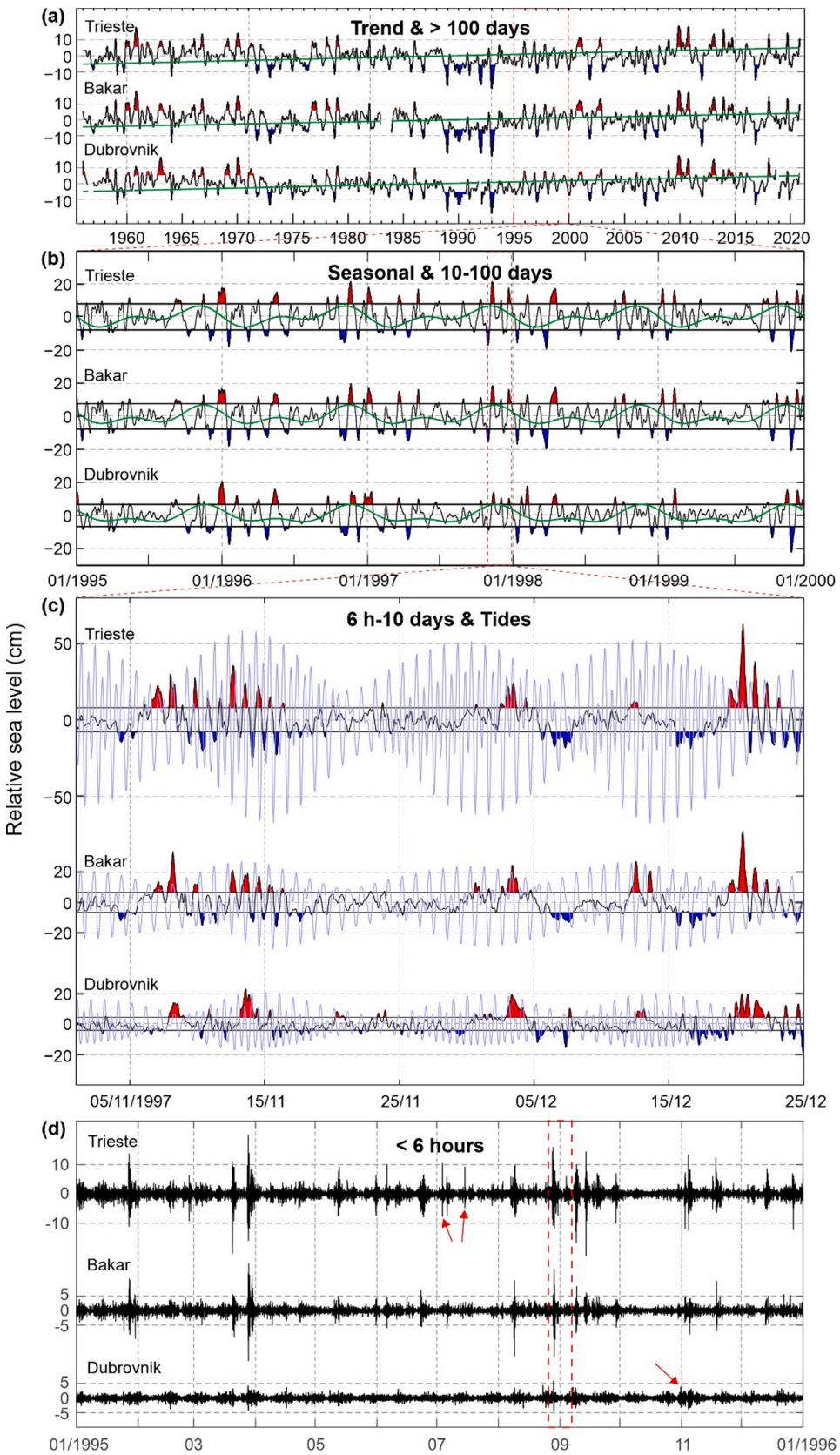

Fig. 10. Decomposition of sea level time series into components: (*a*) *trend* (green) and > 100 *d component* (black); (*b*) *seasonal* (green) and 10–100 *d component* (black); (*c*) 6 *h*-10 *d component* (black) and *tide* (light purple); (*d*) < 6 *h component*. For > 100 *d*, 10–100 *d*, and 6 *h*-10 *d components*, periods during which oscillation were higher (lower) than 1 standard deviation are shaded in red (blue). The red dashed box in (*d*) marks the interval that is magnified in Fig. 12, and red arrows point to the discussed < 6 *h component* episodes. (For interpretation of the references to colour in this figure legend, the reader is referred to the web version of this article.)

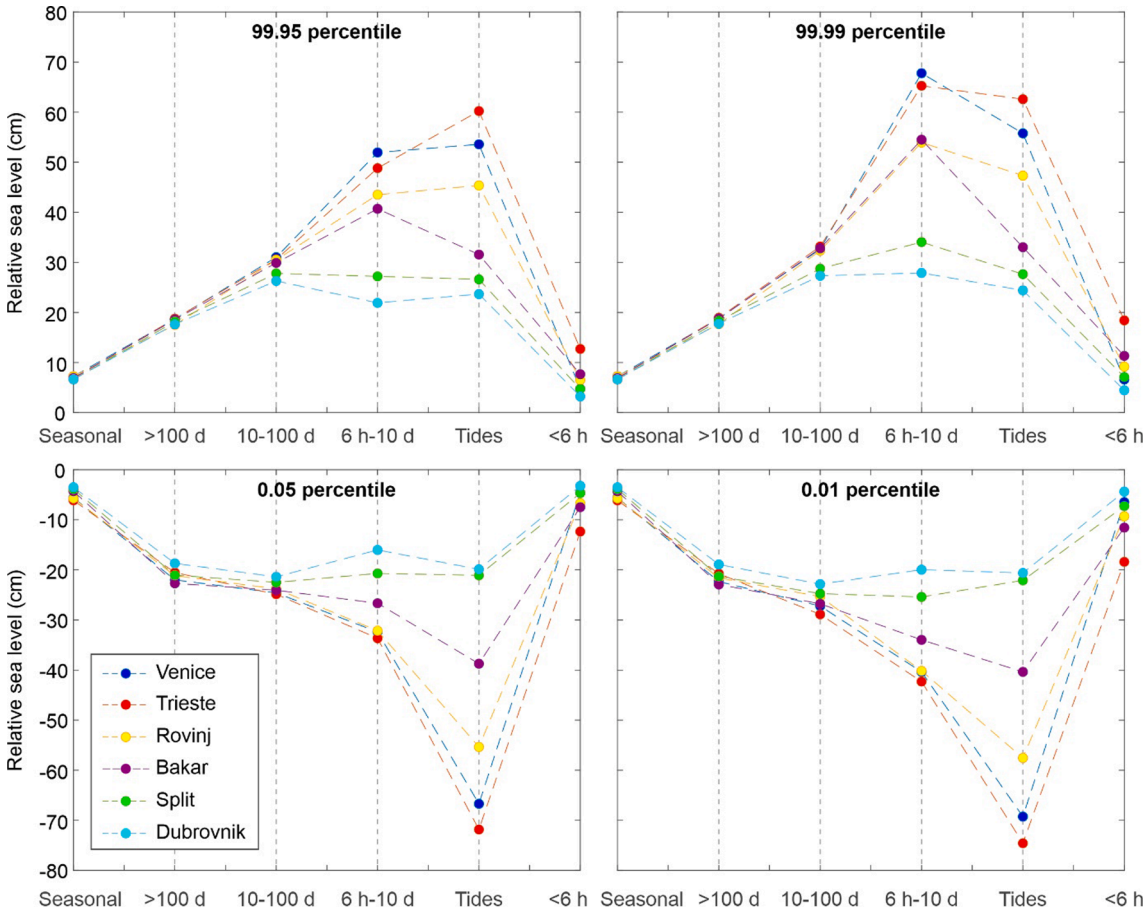

Fig. 11. Values of the 99.95, 99.99, 0.05 and 0.01 percentiles of sea level components at Venice, Trieste, Rovinj, Bakar, Split and Dubrovnik.

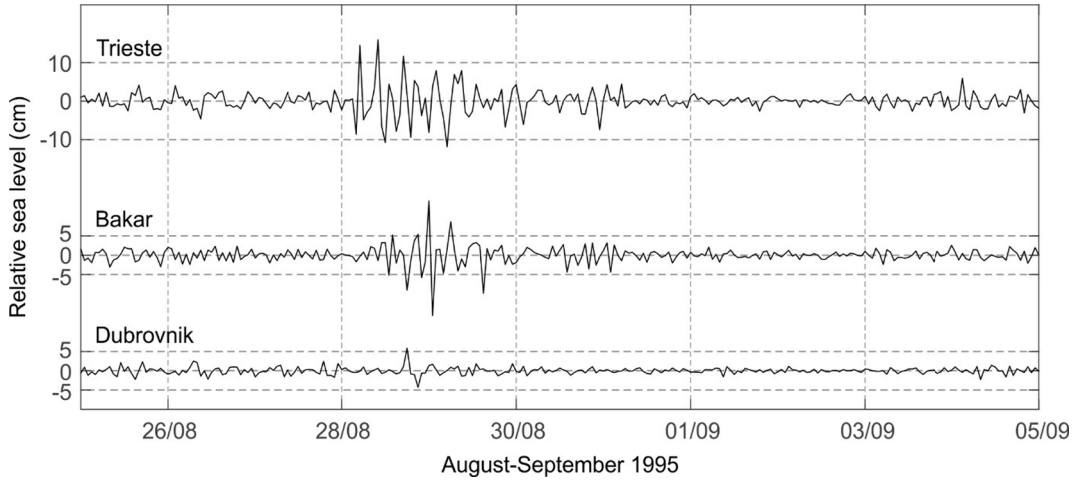

Fig. 12. Time series of < 6 *h component* at Trieste, Bakar, and Dubrovnik – intensified oscillations are seen at all three stations during 28–29 August 1995.

seiches was taken as a process that occurs suddenly, although there are cases of 'continuous quasi-generation' of the oscillations, such as the case from 2009 (Fig. 15 *right*). The process of Adriatic fundamental seiche generation is still not completely understood and is still mostly considered to be excited by rapid changes in winds over the Adriatic (Kasumović, 1963; Cerovečki et al., 1997; Raicich et al., 1999; Leder and Orlić, 2004). However, cyclones and atmospheric fronts need some time to travel over the Adriatic, introducing a complex wind forcing to the seiche that may depart from the theoretical framework. Better individual event representation could be achieved by choosing event-related individual parameters; however, for the purpose of this research, we choose to restrict ourselves to a general set of constants, which results in acceptable estimates.

5.2. *Negative extremes*

The most important contributor to the negative extremes (Fig. 13b) over the shallow northern Adriatic is *tide,* which accounts, on average, for ~58–60% of EN episodes and ~55–65% of HEN episodes height in Venice, Trieste and Rovinj. Going slightly towards the south, i.e., to the

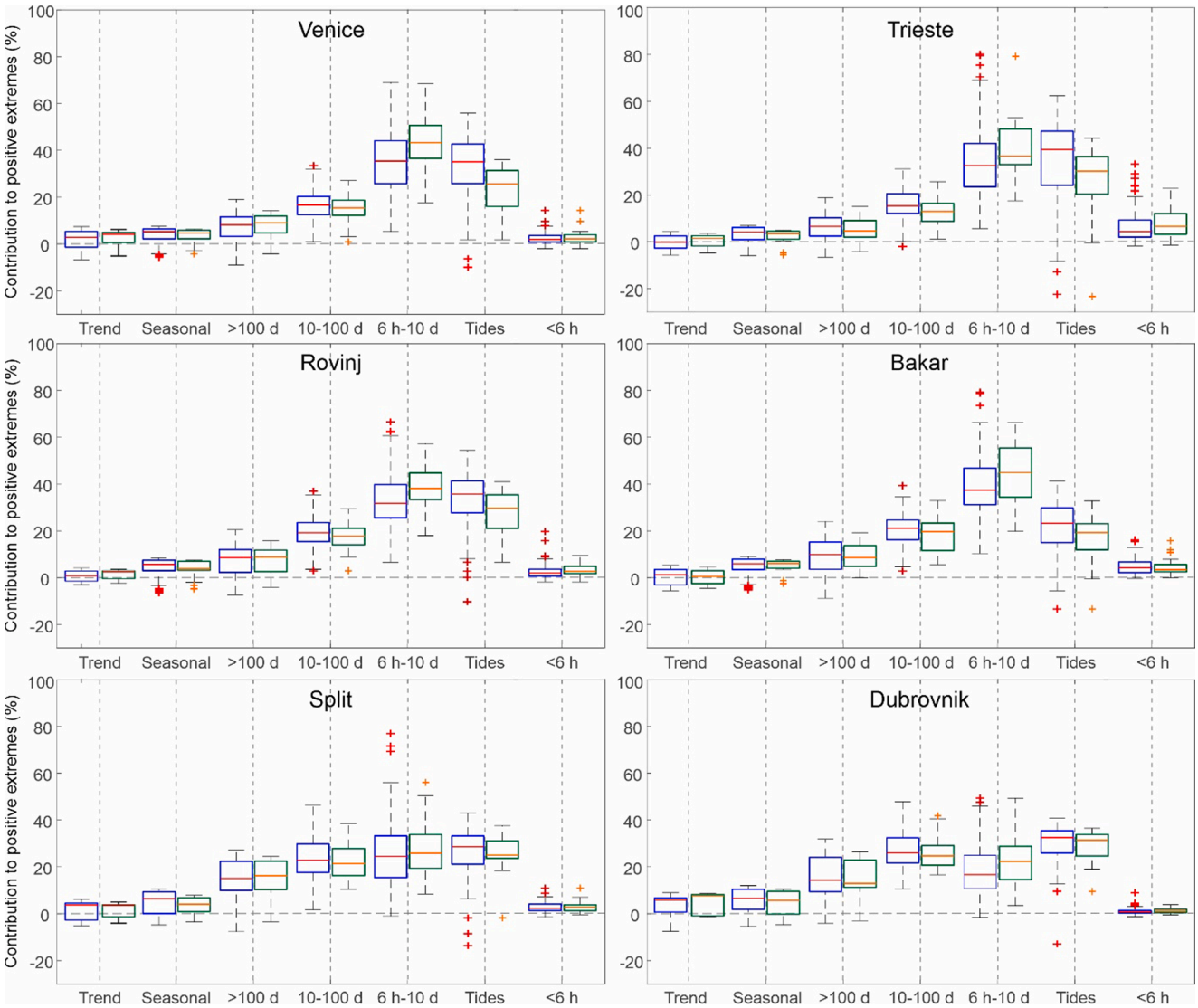

Fig. 13a. Positive extremes – box plots of the percentage of component contributions to positive extremes; the left boxes (blue + red) represent EP episodes; and the right boxes (green + orange) represent HEP episodes. The edges of the boxes represent the 25th and 75th percentiles, while the central line represents the median. Minima and maxima (excluding outliers) are indicated with highest and lowest marks (black). Outliers are marked with crosses. (For interpretation of the references to colour in this figure legend, the reader is referred to the web version of this article.)

Bakar station, the contribution of *tide* weakens, although it is still the most important one (explaining ~45% of the therein EN and HEN episodes). At Bakar, the contribution of other components, primarily the > 100 *d* and 10–100 *d components*, increases, jointly explaining ~40% of both EN and HEN episode heights. More to the south, both in Split and Dubrovnik, the 10–100 *d component* and *tide* are of equal importance, explaining ~60% of EN and HEN episodes in Split and Dubrovnik; these are closely followed by the > 100 *d component* at both stations, explaining up to 25% of EN and HEN episodes at both stations.

At all stations, the contribution of the *trend* to EN and HEN episodes is close to zero, implying that the number of negative extremes is similar during the first and second halves of the studied period (also confirmed by mostly nonsignificant trends; Table 2). The distributions of *seasonal component* contributions to the negative extremes are generally much narrower than the associated distributions related to the positive extremes, aside for Bakar. Mean values of contribution to EN episodes range from ~3 to 5% for both EN and HEN episodes.

For the sea level oscillations at periods shorter than 6 h, their contribution to the negative extremes is mostly negligible (i.e., lower than 6.0%, even when outliers are considered) at all stations aside from Trieste and Bakar. At these two stations, there were a few outlier episodes during which high-frequency sea level oscillation contributed to EN episodes with up to 34.4% (Bakar) and to HEN episodes with up to 26.6% (Trieste).

5.3. *Clustering and simultaneity of extremes*

Episodes of sea level extremes tend to cluster. In Table 3, we give percentages of EP and HEP episodes that occurred within 3 d from each other and of EN and HEN episodes that occurred within 6 d from each other. It is assumed that a time span between episodes longer than the given cut-off periods insures the independence of events. The number of clustered episodes (aside for HEP episodes) increases going from the north towards the south, both for the positive and for the negative extremes. Whereas in Venice 20.4% of EP episodes were clustered, in Dubrovnik 42.0% of EP episodes were clustered. At all stations, negative episodes are clustered more than positive episodes, maintaining a north-to-south gradient. The station that shows the least clustering of negative episodes is Trieste, where 43.7% of EN and 25.8% of HEN episodes occurred within a group, contrary to Dubrovnik, where 81.9% of EN and

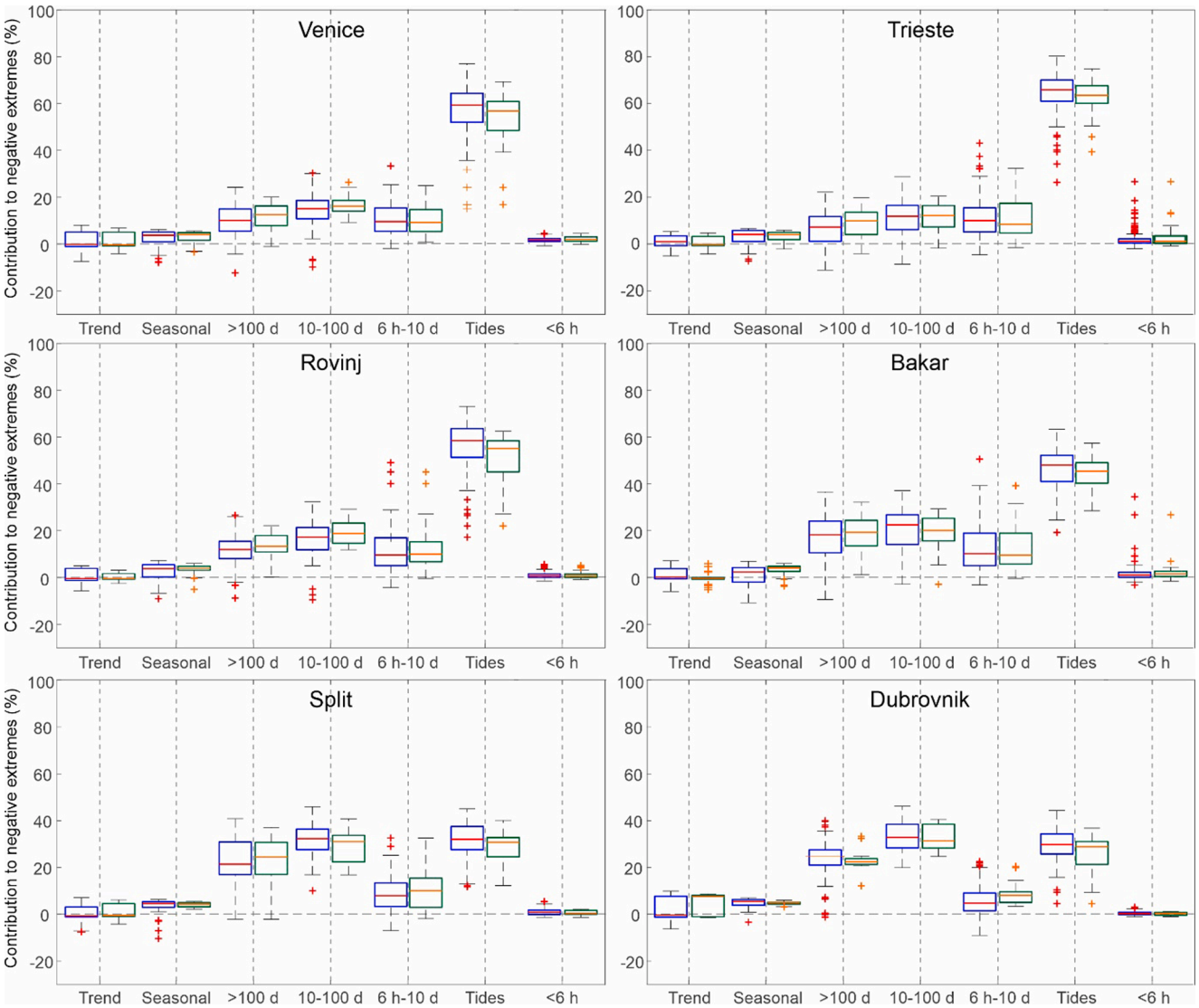

Fig. 13b. Negative extremes – box plots of the percentage of component contributions to negative extremes; the left boxes (blue + red) represent EN episodes; and the right boxes (green + orange) represent HEN episodes. The edges of the boxes represent the 25th and 75th percentiles, while the central line represents the median. Minima and maxima (excluding outliers) are indicated with highest and lowest marks (black). Outliers are marked with crosses. (For interpretation of the references to colour in this figure legend, the reader is referred to the web version of this article.)

75.0% of HEN episodes were clustered. The spatial distribution of clustered episodes again reveals that longer-period components are more important over the middle and southern Adriatic than over the northern Adriatic, and a higher number of clustered negative episodes indicates that the same is true for negative vs positive extremes (Figs. 13a, b).

In Table 3, we also give a median number of episodes and an average time interval between the episodes occurring within a group for each station and for each type of episode. At all stations, the median number of episodes within a cluster was 2–2.5 for the positive extremes, not changing significantly from the north towards the south and from EP to HEP episodes. For the negative extremes, the median number of episodes within a cluster increases from the north towards the south and from HEN to EN episodes, reaching median values of 5 episodes per cluster in Split and 6 in Dubrovnik for EN episodes. The largest number of episodes within the cluster was recorded during February 1959, when 10 subsequent EN episodes occurred in Split and 19 in Dubrovnik. The observed increase in the number of clustered episodes and in the number of episodes per clustered group over the middle and southern Adriatic is likely, as stated above, since the 10–100 *d component* contributes more to the extremes therein than over the northern Adriatic (Fig. 13b). The median time interval between two episodes within the cluster was 24.0 h for all stations and for all types of episodes. Exceptions were only HEP in Venice (48.0 h) and Rovinj (36.0 h). The 24.0 h duration implies that maxima (and minima) of subsequent episodes are mostly concurrent with the diurnal maxima of *tide* possibly joined with the Adriatic seiche.

In Fig. 16, we show a simultaneity index that is defined for each pair of tide gauge stations as a percentage of situations during which maxima of EP (EN) episodes appeared at both stations within a $\tau = 3$ (6) d limit, implying that an episode at one station occurs at most 3 (6) d before or after an episode at another station. We noticed two areas of simultaneity: the northern Adriatic (Venice, Trieste, Rovinj, and Bakar) and the middle/southern Adriatic (Split, Dubrovnik). Over each of these areas, positive episodes were likely to occur in $> 60\%$ of situations at the area stations, with the percentage rising to $> 80\%$ over the very northern Adriatic (Venice, Trieste and Rovinj). The chance for a simultaneous occurrence of positive extremes over both the northern and the middle/southern Adriatic is lower, having likelihoods of 20–60%. For the negative extremes, the same simultaneity areas can be noticed; however, the chance of negative extremes occurring simultaneously over any pair

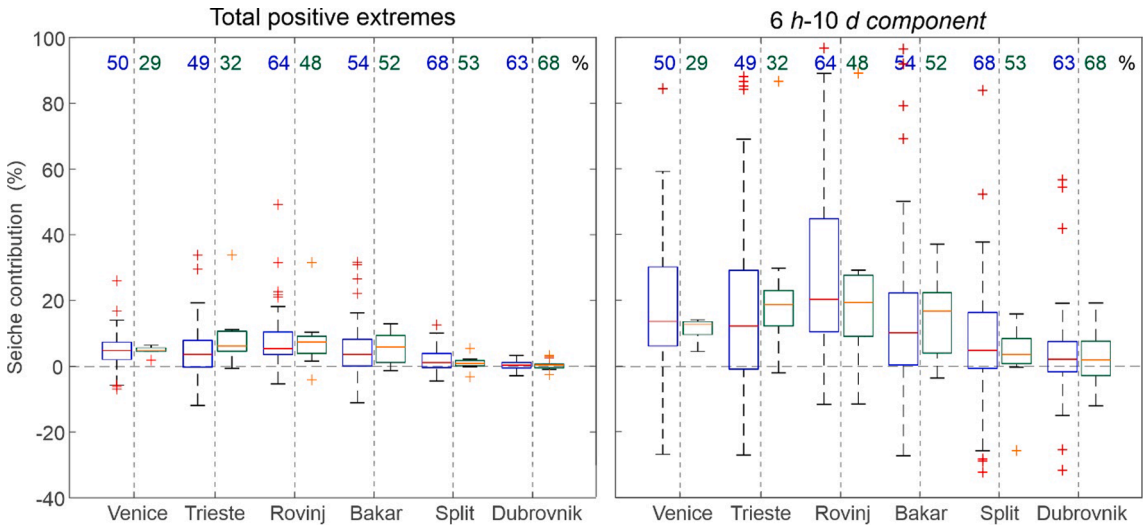

Fig. 14. Box plots of seiche contribution to (*left*) total extremes and to (*right*) 6 *h*-10 *d component* of total extremes. The numbers at the top represent the percentage of extreme situations with previously excited seiche.

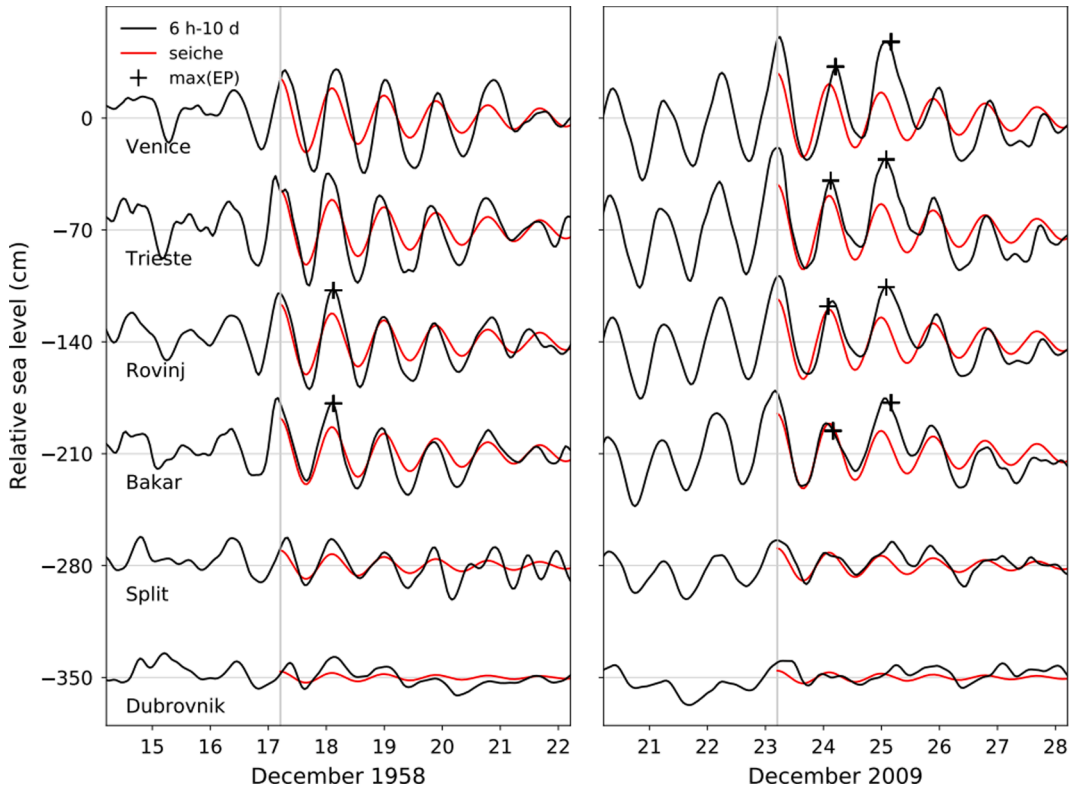

Fig. 15. 6 *h*-10 *d component* of sea level series during three floods: (*left*) 17 December 1958 and (*right*) 24/25 December 2009, with previously excited seiches indicated. Estimated seiches are shown with red lines. Time of extreme maxima influenced by preexisting seiche are marked with black crosses (only at those stations at which event was at least EP episode). Vertical grey lines indicate the onsets of seiches. (For interpretation of the references to colour in this figure legend, the reader is referred to the web version of this article.)

of stations is usually higher than it is for positive extremes. Additionally, the negative extremes that occur synchronously over the entire Adriatic are more likely than the positive extremes. This was to be expected as, in addition to tidal oscillations, the negative extremes are governed by longer period sea level components (10–100 *d*, > 100 *d component*) (Fig. 13b), which behave quasi-uniformly over the entire Adriatic (Fig. 10 and Fig. 11). In contrast, the positive extremes are governed by shorter period components and mostly by the 6 *h*-10 *d component* (Fig. 13a), which changes significantly from the south towards the north, both in regard to the amplitude and shape of sea level oscillations (Fig. 10 and Fig. 11) and by tidal oscillations for which the semidiurnal component is in the counterphase between the two areas (Medvedev et al., 2020). Interestingly, the matrix of the simultaneity index is not symmetrical: a chance, e.g., for an EN episode to occur in Trieste within 6 d of an EN episode occurring in Split (84%), was much higher than a chance for an EN episode to occur in Split within 6 d of an EN episode occurring in Trieste (36%). This is because the episodes in Split were more clustered and, thus, usually a higher number of Split episodes was

Table 3
Percentage of clustered episodes (%), median number of episodes within a group (No.), median time interval between extremes within clustered episodes.

	HEP (99.99)			EP (99.95)			HEN (0.01)			EN (0.05)		
	%	No.	T (h)	%	No.	T (h)	%	No.	T (h)	%	No.	T (h)
Venice	23.8	3	48.0	20.4	2	24.0	47.1	3	24.0	51.9	3	24.0
Trieste	22.6	2.5	24.0	24.3	2	24.0	25.8	2	24.0	43.7	3	24.0
Rovinj	17.4	2	36.0	29.0	2	24.0	50.0	2	24.0	55.1	3	24.0
Bakar	26.1	2	24.0	23.5	2	24.0	41.4	2	24.0	55.4	3.5	24.0
Split	13.3	2	24.0	33.77	2	24.0	52.9	3.5	24.0	69.4	5	24.0
Dubrovnik	22.7	2	24.0	42.0	2.5	24.0	75.0	3	24.0	81.9	6	24.0

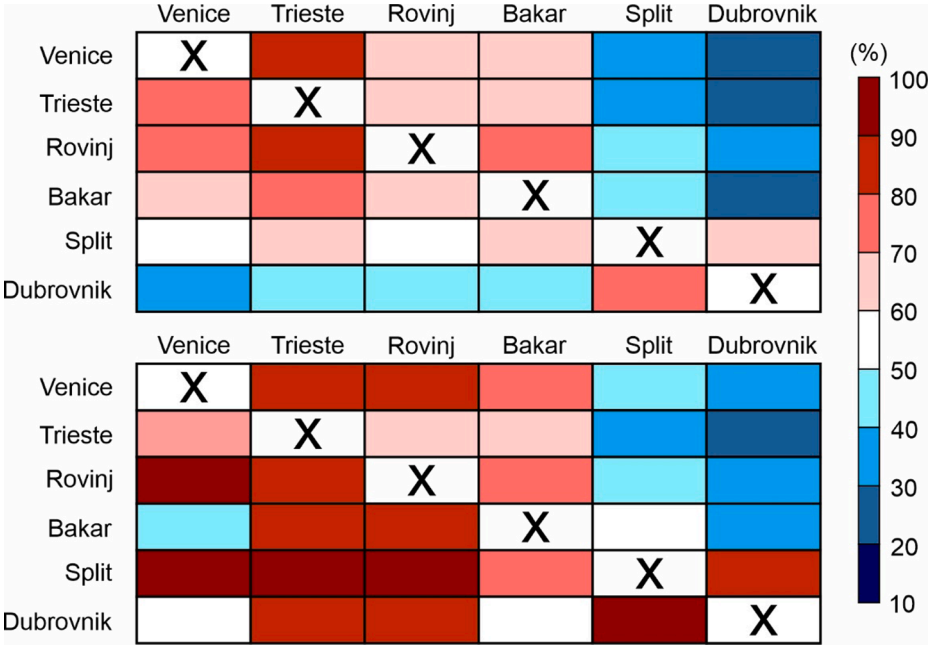

Fig. 16. Simultaneity index (percentages of episodes occurring at two stations within a prescribed interval) of (*upper*) EP episodes and (*bottom*) EN episodes. The simultaneity index is not defined for same-station pairs (marked with "X").

associated with one Trieste episode. In contrast, Trieste episodes were spread more evenly throughout the studied period (Fig. 6; Table 3).

6. Discussion

The Adriatic sea levels are known to reach extreme heights, are highest in the Mediterranean, and cause severe flooding (Marcos et al., 2009; Cavaleri et al., 2020). The anticipated climate change and associated mean sea level rise are likely to make these events even more hazardous (Merrifield et al., 2013). A sea level rise of 40–60 cm along the European coasts might result in a present-day 100-year return level becoming a 3-year return level by 2100 (Vousdoukas et al., 2017), providing that the underlying atmospheric and hydrological processes and tidal oscillations retain their present-day climatology. The analysis presented herein already implies that trends in the duration of EP and intensity of HEP sea level extremes up to 2020 are positive (Table 2).

To deduce what will happen in the future, we first need to understand what sea level oscillations and to what extent cause present-day extreme sea levels. By decomposing the measured sea level into seven distinct components, each of which is primarily, but not uniquely, governed by different atmospheric/ocean processes, we quantified the contributions of these components to the eastern and northern Adriatic sea level extremes. We have shown that there are significant differences between positive and negative extremes and between the northern and the middle/southern Adriatic. The question that needs to be addressed in detail in subsequent studies is to what extent the observed spatial distribution is governed by spatial changes in atmospheric (including air-sea fluxes), thermohaline, hydrologic and geological processes over the Adriatic and to what extent it is governed by topographic effects, i.e., by the fact that the Adriatic Sea is a narrow bay that strongly shallows towards the north (Fig. 1).

As an intro into the proposed further research, we look at the spatial distribution of relevant atmospheric variables. In Fig. 17, we show percentiles of hourly time series of mean sea level pressure (MSLP) and 10-m wind speed components, all obtained from the ERA5 data at the points closest to our tide gauge locations, for the 1979 to 2020 period. The south-to-north variability of MSLP, although existent, is much less pronounced than the corresponding sea level variability, and the analysed wind series do not show a clear south-to-north variability. Slightly stronger MSLP variability over the northern Adriatic is due to the northern Adriatic being closer to the cyclogenesis area of the Gulf of Genoa, whereas winds clearly have a more changeable spatial structure, which is related to the local topography as well as to the MSLP fields (Ulbrich et al., 2012). Since the spatial variability of the atmospheric forcing is not pronounced, it implies that the differences between the northern and the middle/southern Adriatic originate from other sources as well. One of the key reasons for the observed spatial distribution is certainly the topographic enhancement of sea level oscillations, i.e., of *tide* and the 6 *h*-10 *d component* over the shallow northern Adriatic (Polli, 1959; Orlić et al., 1994; Bertotti et al., 2011). However, other reasons, such as circulation changes (including coastal currents) (e.g., Pujol and Larnicol, 2005), cross-shore wind jets (e.g., Orlić et al., 1994), effects of freshwater sources (rivers) and water fluxes (e.g., Volkov and Landerer, 2015), might play a significant role – a topic to be studied in more detail.

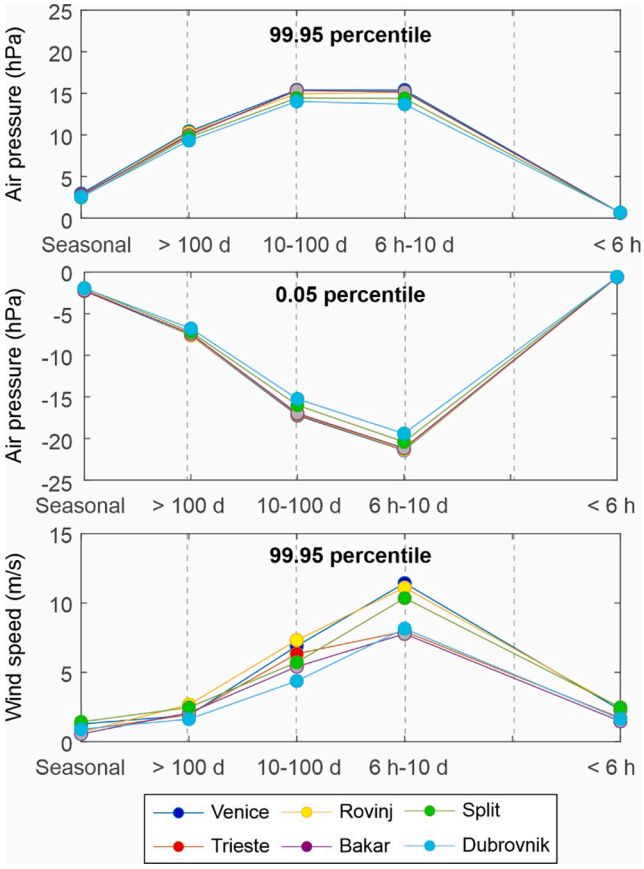

Fig. 17. Variability of atmospheric forcing (*upper*) 99.95 percentile value of the MSLP components; (*middle*) 0.05 percentile value of the MSLP components; (*bottom*) 99.95 percentile value of wind speed components; all for the ERA5 hourly values (1979–2020) at the grid points closest to the tide gauge locations.

Future characteristics and trends relevant for the Mediterranean (and the Adriatic) positive sea level extremes have been researched for some processes. Naturally, most attention has been dedicated to storm surges (within the 6 *h*-10 *d component*) and governing atmospheric extratropical cyclones. The frequency and intensity of these cyclones were generally found to weaken over the Mediterranean and the Adriatic Sea during the last decades of the 20th century (Trigo and Davies, 2002), reflecting also the occurrence and intensity of storm surges (Androulidakis et al., 2015). For the future, climate projections for storm surges are still uncertain, although they point to either steadiness or a decrease in their frequency and duration (Lionello et al., 2012; Šepić et al., 2012b; Mel et al., 2013; Androulidakis et al., 2015; Denamiel et al., 2020). The surges are also characterized by a spatial difference in their maxima caused by spatial variations in the sirocco wind and bathymetry (Međugorac et al., 2018), for which no changes in the future climate have been projected (Međugorac et al., 2020). Changes in *tide* due to anticipated climate change have also been studied: the tides appear to be sensitive to mean sea level changes, with the rise of the Adriatic sea level of > 2 m projected to change the tidal amplitudes. However, such a rise is unlikely by 2100, and first projections are uncertain: depending on the levels of mean sea level rise and coastal protection, the related amplitude change might be either positive or negative (Lionello et al., 2005). For the 10–100 *d component*, there are no available projections in the Mediterranean, yet planetary waves are expected to weaken and be pushed poleward in the future climate (Wills et al., 2019) with fewer blocking situations (Woollings et al., 2018), which might result in a weakening of this component.

Another pressing question is how large can total sea level extremes become. We and other authors (for positive events only, e.g., Marcos et al., 2009) have given an initial answer to this question by estimating the return levels of hourly sea level time series. Our analysis provides an opportunity to look at this question from a different angle as well – how high (low) extreme sea levels would be if they occurred due to all components reaching maximum (minimum) values simultaneously. Comparison of maxima, minima, 99.99 and 0.01 percentiles of the original time series to sums of maxima, minima, 99.99 and 0.01 percentiles of the six individual components (excluding trend which can be added linearly) is given in Table 4. At all stations, sums of maxima and 99.99 percentiles derived from the components give significantly higher values than the maxima and 99.99 percentiles of the original time series. If we, e.g., look at the Rovinj station, we notice that the observed total maximum is 114.7 cm, whereas the sum of the maxima of all six components is 202.3 cm – a 76.4% higher value. At other stations, these differences range from 56.3% (Venice) to 78.0% (Dubrovnik). Regarding the negative values, the differences between the minima and 0.01 percentiles of the original time series and minima and the 0.01 percentiles estimated as sums of the components are even more pronounced. The recorded minimum at Trieste is −119.2 cm, whereas the sum of the recorded minima of all six components is −247.5 cm, which is a 107.6% lower value. At other stations, sums of estimated minima of components differ from the recorded minima of time series between 71.5% (Dubrovnik) and 104.1% (Bakar). Given that most (but not all) components reach their maximum (minimum) values during the same months (Fig. A1, Appendix A), our analysis imply that even more extreme floods could be reached – how much is yet another open research question. Ferrarin et al. (2022) attempted to answer these questions by applying a methodology similar to ours to time series measured in Venice during 1872–2019 (series consist of up to 4 values per day up to 1939; hourly series up to 2009, and 10-min series up to 2019). They decomposed detrended time series into five components similar, but not identical, to ours and showed that, in particular, synoptic component (storm surge and seiche in Ferrarin et al., 2022) is unlikely to reach its maxima values during maxima of tide – a feature for which no clear explanation is offered yet.

The fact that extreme sea levels would potentially be much higher (lower) if tidal and synoptic maxima occurred at the same times is also suggested by some historic extreme episodes. The first was the great flood of 4 November 1966, during which the highest ever sea level was recorded in Venice (167.5 cm). According to Međugorac et al. (2015) and our analyses, the flood occurred dominantly due to the extremely high 6 *h*-10 *d component* (storm surge) with all the other components rather weak during the event, including *tide,* which was close to the low

Table 4
Maximum, minimum, 99.95, 99.99, 0.05 and 0.01 percentiles (cm), as determined from the original time series and as determined from the sum of six analysed components.

	TS_{max}	$\sum_{i=1}^{6} Comp_{max}$	TS_{min}	$\sum_{i=1}^{6} Comp_{min}$	$TS_{99.99}$	$\sum_{i=1}^{6} Comp_{99.99}$	$TS_{0.01}$	$\sum_{i=1}^{6} Comp_{0.01}$
Venice	167.5	261.8	−116.5	−205.7	115.6	188.9	−99.5	−171.2
Trieste	182.7	294.1	−119.2	−247.5	115.8	205.2	−102.2	−191.0
Rovinj	114.7	202.3	−97.3	−191.9	94.7	168.1	−85.3	−158.7
Bakar	111.5	190.1	−82.5	−168.4	88.4	157.3	−69.6	−139.9
Split	85.4	147.3	−64.6	−122.4	70.4	122.1	−54.6	−103.9
Dubrovnik	74.0	131.7	−61.0	−104.6	63.0	108.5	−53.0	−90.2

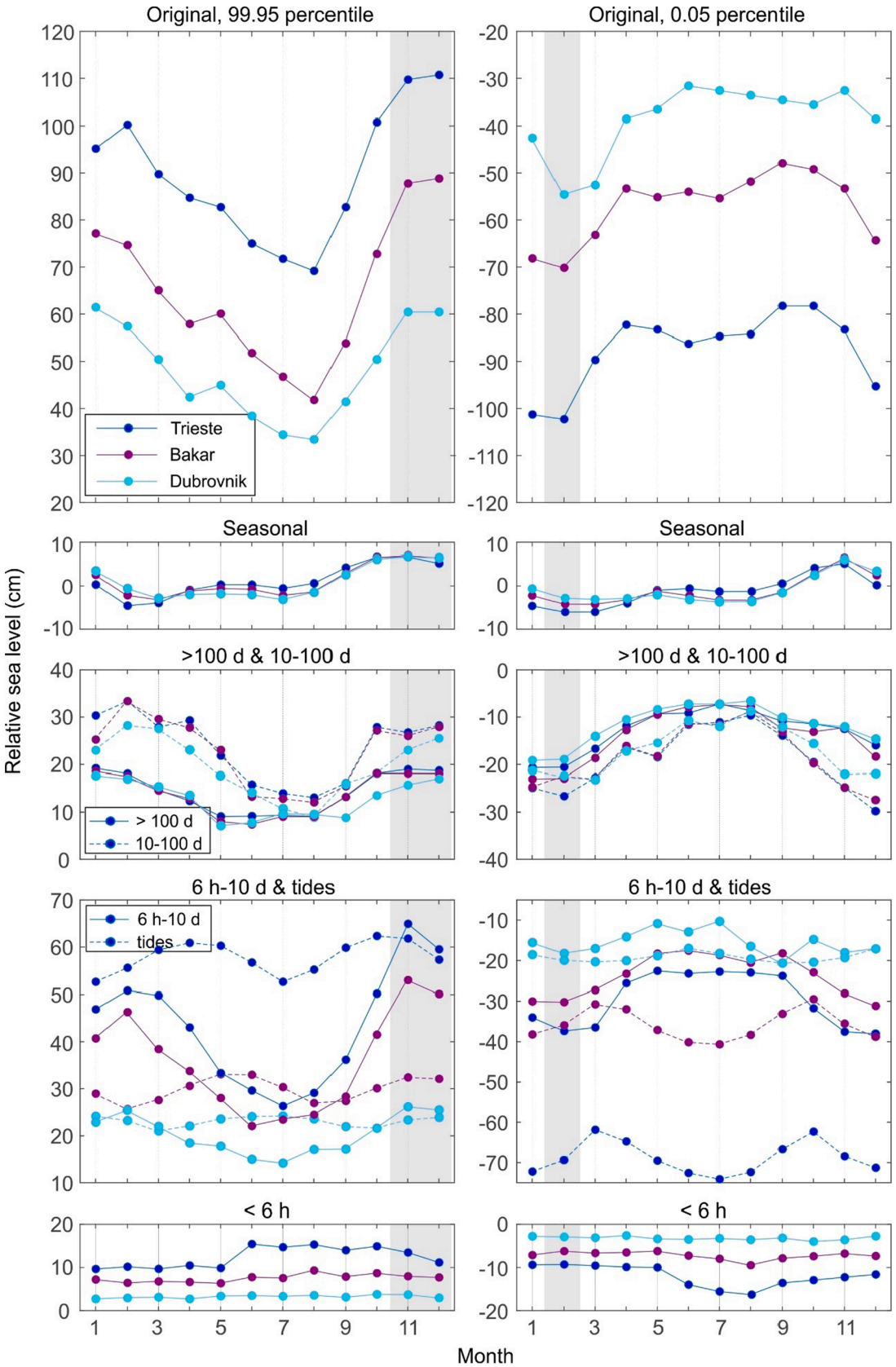

Fig. A1. Seasonal distribution of the 99.95 and 0.05 percentiles of sea level heights for the original time series and for six studied components for the Trieste, Bakar and Dubrovnik time series.

water. Were the tidal oscillations at their peak (i.e., if maximum of storm surge occurred just 5 h earlier), the flood would be ~40 cm higher, and the resulting sea level would be higher than the herein estimated 100-year return value (170.8 cm) by the astonishing ~37 cm. The second example is the more recent Venice flood on 12 November 2019. During this event, sea levels reached a height of 156.5 cm, only 11 cm less than during the 1966 event, classifying it as the second largest flood of the instrumental period (Cavaleri et al., 2020). This flood was the result of superposition of the already increased Mediterranean-wide sea level (> 10 d), storm surge (within 6 *h*-10 *d component*), *tide* (flood occurred close to the high water) and, unexpectedly, of the higher frequency sea level oscillation (T < 6 h) related to a propagation of a relatively small (O (10–100 km)) fast moving atmospheric depression coming from the southern Adriatic, which added ~20 cm to the already increased sea level. However, the extreme occurred during lower high water (Ferrarin et al., 2021), which was in fact 20 cm lower than the higher high water 12 h earlier and later – if the event happened during the higher high water, it would have surpassed the record-breaking extreme of 4 November 1966.

Although our analysis suggests that the < 6 *h component* is mostly negligible in regard to extreme sea levels, the case of the 12 November 2019 Venice flood suggests that it can, however, have a profound effect on extreme sea levels, even at those locations at which it is normally not significant (Cavaleri et al., 2020). This is even more so at those locations at which this component is strong. High-frequency sea level oscillations related to the Gulf of Trieste seiche contributed to the record setting Trieste flood of 26 November 1969 (182.7 cm) (Table 4) with 39.8 cm, making this component the second largest single contributor to the flood (after synoptic component with 96.9 cm). The highest sea level (analysed in our study) related to the < 6 *h component* was recorded in Trieste on 30 August 1992 and was 60.3 cm. Although on this occasion, the total sea level did not reach extreme heights (95.8 cm), it should be noted that the < 6 *h component* was pronounced for a duration of almost 7 consecutive days and that on 4 September 1992, the Trieste Bay oscillations coincided with a northern Adriatic meteotsunami recorded at the nearby Rovinj station (Šepić et al., 2012a). Let us also mention that the hourly sea level data are obtained by digitization done in such a way that all sea level oscillations at periods shorter than 2 h are filtered out. To obtain a better understanding of the contribution of sea level oscillations with periods up to 1–2 min, we examined original mareographic charts of all EP and HEP episodes from Rovinj and Bakar tide gauges, two locations for which these charts were available, and at which high-frequency sea level oscillations can be rather strong (Goldberg and Kempni, 1938; Šepić et al., 2008; Šepić et al., 2012a). The average differences between maxima read directly from charts and maxima of digitised hourly time series, all during the EP episodes, were 4.7 cm at Rovinj and 9.0 cm at Bakar, with maximum differences of 35.7 cm at Rovinj and 44.3 cm at Bakar. Furthermore, we must keep in mind that over some parts of the Adriatic Sea, the < 6 *h component* can be so strong during individual meteotsunami events that it can surpass even the highest (and lowest) extreme sea levels analysed here. During the 1978 Great Flood of Vela Luka, sea level oscillations of ~20 min period reached astonishing 6 m wave height, completely flooding the otherwise well protected embayment. At nearby Split and Dubrovnik tide gauges, short-period (< 2 h) sea level oscillations recorded during this event had amplitudes of 23 and 18 cm, respectively (Orlić et al., 2010). Oscillations of such short periods with ranges above 3 m have also been observed at a few other Adriatic locations several times within the last 100 years (Orlić, 2015; Šepić et al., 2022). Clearly, oscillations at periods shorter than 2 h can significantly contribute to total sea levels, as already documented for Trieste for all events (Tsimplis et al., 2009) and for selected Adriatic stations for meteotsunami events (Orlić, 2015; Šepić et al., 2022). We therefore finish our discussion with a strong hope that the subhourly (preferably 1-min) sea level data will become of sufficient quality and spatial distribution in the future so that sea level extremes can be studied within their full scope and that related analysis will be included in all relevant hazard studies.

7. Conclusions

The following conclusions related to (1) the total sea level extremes; (2) the general properties of the sea level components and their extremes; and (3) the contribution of the sea level components to the total sea level extremes can be reached.

Total sea level extremes:

(1) Positive (negative) sea level extremes have a strong south-to-north gradient, with median daily maxima (minima) of the positive (negative) extremes over the northern Adriatic 2–2.5 times higher (lower) than over the middle and the southern Adriatic.
(2) The estimated return values of positive and negative extremes are 1.5–2.5 times larger over the northern than over the southern Adriatic.
(3) Total sea level extremes have a pronounced seasonal distribution, with most of the positive extremes occurring during November and December over the entire Adriatic and most of the negative extremes occurring during January to February over the northern Adriatic and during February to March over the middle and the southern Adriatic.
(4) Trends in the number of extremes, their duration and intensity point to prolongation of EP episodes and strengthening of HEP episodes over most stations. Other trends are mostly insignificant.
(5) Yearly rates of occurrence of extremes revealed a strong decadal variability with at least three periods of several years length during which either positive or negative extremes dominated the time series.

General properties of the sea level components and their extremes:

(1) The strongest positive components over the northern Adriatic are *tide* and 6 *h*-10 *d component*, and over the middle and the southern Adriatic 10–100 *d*, 6 *h*-10 *d*, and *tide*.
(2) The strongest negative component over the northern Adriatic is *tide*; over the middle and the southern Adriatic, > 100 *d*, 10–100 *d*, 6 *h*-10 *d* and *tide* components are of comparable strength.
(3) *Trend* is positive at all stations, but over the entire period, its contribution to the total height of extremes is close to zero.
(4) The entire Adriatic Sea oscillates uniformly (same phase and amplitude) at periods longer than 100 d.
(5) *Seasonal component,* as well as 10–100 *d component*, are in phase over the entire Adriatic, but with amplitudes that slightly increase towards the north.
(6) 6 *h*-10 *d* and *tide*, are not in phase over the Adriatic Sea. A pronounced south-to-north gradient is evident - amplitudes of these components are up to 3 times larger over the northern than over the southern Adriatic.
(7) 6 *h*-10 *d component* has strong variability; this variability is more pronounced over the northern Adriatic and is also more pronounced for the positive than for the negative extremes.
(8) < 6 *h component* is characterized by the smallest amplitudes, which have no clear south-to-north gradient.

Contribution of the sea level components to the total sea level extremes:

(1) Components that contribute the most to the total positive extremes over the northern Adriatic are 6 *h*-10 *d component* and *tide*, with 6 *h*-10 *d* component found to be the most important contributor to the highest (HEP) episodes.
(2) Over the middle/southern Adriatic, 10–100 *d component*, 6 *h*–10 *d component*, and *tide* contribute evenly to the total positive extremes.

(3) The Adriatic seiche contributes significantly to the positive extremes over the northern Adriatic, occasionally explaining > 90% of 6 *h*–10 *d component*.
(4) The most important contributor to the negative extremes over the northern Adriatic is *tide*.
(5) Over the middle and southern Adriatic, 10–100 *d component* and *tide* contribute evenly to the negative extremes, closely followed by > 100 *d component*.
(6) < 6 *h* and *seasonal components* contribute the least to both positive and negative Adriatic sea level extremes.

Declaration of Competing Interest

The authors declare that they have no known competing financial interests or personal relationships that could have appeared to influence the work reported in this paper.

Data availability

Data availability statement is added to the manuscript. Links to data repositories are given, as well as links to agencies which own used data.

Acknowledgements

We thank the personnel of the Hydrographic Institute of the Republic of Croatia and Department of Geophysics, Faculty of Science, University of Zagreb, the Istituto Superiore per la Protezione a la Ricerca Ambientale, the Institute of Marine Sciences of the National Research Council of Italy and the Centro Previsioni e Segnalazioni Maree for their diligent maintenance of the tide gauges and for continuous digitization of sea level data. We personally thank Fabio Raicich (CNR ISMAR - Institute of Marine Sciences) for helping us obtain sea level time series from Trieste and Davide Zanchettin (Ca' Foscari University of Venice) and Christian Ferrarin (CNR ISMAR - Institute of Marine Sciences) for helping us obtain sea level time series from Venice. We also thank the reviewer whose thoughtful comments resulted in a much-improved manuscript. This research has been supported by the ERC-StG project 853045 SHExtreme and by the Croatian Science Foundation projects IP-2019-04-5875 StVar-Adri, IP-2018-01-9849 MAUD and IP-2016-06-1955 ADIOS.

Data availability

Hourly sea level series measured in Venice for the time interval 1983-2020 are available at https://www.comune.venezia.it/node/6214. Older Venetian data (1956-1982) were put at our disposal by Christian Ferrarin (CNR ISMAR Institute of Marine Sciences). Hourly sea level time series measured in Trieste from 1939 to 2018 are available at the SEANOE database (https://doi.org/10.17882/62758). Additional Trieste data (2019-2020) were taken from UHSLC (http://uhslc.soest.hawaii.edu/data/?fd). Hourly sea level time series measured in Bakar are publicly available at the SEANOE database (https://doi.org/10.17882/85171). Hourly sea level time series measured at Rovinj, Split and Dubrovnik should be requested from the Hydrographic Institute of the Republic of Croatia (www.hhi.hr; contact: office@hhi.hr). To our experience and to the best of our knowledge, all of the abovementioned institutions provide hourly sea level time series freely for scientific research.

Appendix A. . Seasonal distributions of extremes of the sea level components

For each component and for each month of the year, we determined its 99.95, 99.99, 0.05 and 0.01 percentile values. The results of our analysis for representative stations (Trieste, Bakar and Dubrovnik) and for the 99.95 and 0.05 percentiles are shown in Fig. A1.

Regarding the positive extremes, it was immediately evident that most of the components have seasonal distributions comparable to the seasonal distribution of the positive extremes of the original time series, with maxima values reached in November and December. Exceptions are the 10–100 *d component,* for which maximum values are reached in February over the northern Adriatic, and *tide,* for which two yearly maxima, out of phase over different parts of the Adriatic Sea, exist. In Trieste, the *tide* reaches its maximum amplitude in April and October, in Bakar in May-June and November, and in Dubrovnik in July and January. Oscillations at periods shorter than 6 h do not have pronounced seasonal distributions and appear evenly throughout the year. The exception is the Trieste tide gauge station, where both positive and negative < 6 *h component* oscillations are stronger during the summer season (June-August).

For the negative extremes, the seasonal distribution of components is again similar to the seasonal distribution of the original extremes, with minima reached from January to March. However, there are some pronounced exceptions. The lowest values of the 0.05 percentile of the 10–100 *d component* are reached in December at all stations, of the 6 *h*-10 *d component* in September in Dubrovnik, and in December in Bakar and Trieste, and of the *tide* in July in Trieste and Bakar, and in September in Dubrovnik.

Appendix B. . Duration of extremes of the sea level components

From the time series of each component, we extract positive extreme episodes as continuous periods of time during which the corresponding (component) sea level surpassed its 99.95 or 99.99 percentile and negative ones as periods of times during which the (component) sea level was lower than its 0.05 and 0.01 percentile. The median duration of all extreme episodes defined in this way is given in Tables B1a and B1b. As expected, the longest extreme duration was achieved for > 100

Table B1a
Median duration (h) of positive extremes of original sea level time series and of analysed components of sea level time series. The number of episodes is included in brackets.

		Venice	Trieste	Rovinj	Bakar	Split	Dubrovnik
99.95 percentile	All	2.0 (103)	2.0 (136)	2.0 (93)	2.0 (102)	3.0 (77)	3.0 (88)
	seasonal	4.0 (59)	4.0 (59)	4.0 (58)	4.0 (58)	4.0 (59)	4.0 (58)
	> 100 *d*	136.0 (1)	259.0 (1)	129.0 (2)	259.0 (1)	259.0 (1)	259.0 (1)
	10–100 *d*	51.0 (4)	65.0 (3)	88.0 (3)	95.0 (3)	66.5 (4)	66.0 (4)
	6 *h*-10 *d*	5.0 (52)	3.0 (69)	4.0 (63)	4.0 (61)	3.0 (84)	3.0 (80)
	tide	1.0 (216)	1.0 (232)	1.0 (218)	1.0 (199)	1.0 (202)	1.0 (235)
	< 6 *h*	1.0 (243)	1.0 (254)	1.0 (250)	1.0 (256)	1.0 (248)	1.0 (251)
99.99 percentile	all	2.0 (21)	1.0 (31)	2.0 (23)	2.0 (23)	2.0 (15)	2.0 (22)
	seasonal	1.0 (51)	1.0 (37)	1.0 (38)	1.0 (5)	1.0 (32)	1.0 (34)
	> 100 *d*	27.0 (1)	52.0 (1)	52.0 (1)	52.0 (1)	52.0 (1)	52.0 (1)
	10–100 *d*	13.5 (2)	52.0 (2)	26.0 (2)	26.0 (2)	26.0 (2)	52.0 (1)
	6 *h*-10 *d*	3.0 (14)	4.0 (15)	3.0 (17)	4.0 (14)	2.5 (20)	3.0 (18)
	tide	1.0 (47)	1.0 (49)	1.0 (49)	1.0 (41)	1.0 (41)	1.0 (52)
	< 6 *h*	1.0 (51)	1.0 (52)	1.0 (50)	1.0 (52)	1.0 (50)	1.0 (52)

Table B1b
Median duration (h) of negative extremes of original sea level time series and of analysed components of sea level time series. The number of episodes is included in brackets.

		Venice	Trieste	Rovinj	Bakar	Split	Dubrovnik
0.05 percentile	all	2.0 (131)	2.0 (158)	2.0 (127)	2.0 (121)	3.0 (72)	3.0 (83)
	seasonal	4.0 (59)	4.0 (59)	4.0 (58)	4.0 (58)	4.0 (59)	4.0 (58)
	> 100 *d*	68.0 (1)	259.0 (1)	129.0 (1)	129.5 (1)	129.5 (1)	259.0 (1)
	10–100 *d*	68.0 (4)	52.0 (4)	42.0 (5)	63.0 (4)	33.0 (5)	53.0 (4)
	6 *h*-10 *d*	3.0 (80)	3.0 (81)	3.0 (86)	3.0 (81)	2.0 (101)	3.0 (84)
	tide	1.0 (224)	1.0 (226)	1.0 (217)	1.0 (202)	1.0 (215)	1.0 (233)
	< 6 *h*	1.0 (246)	1.0 (249)	1.0 (248)	1.0 (256)	1.0 (245)	1.0 (245)
0.01 percentile	all	1.0 (34)	1.0 (31)	2.0 (30)	2.0 (29)	2.5 (17)	2.0 (16)
	seasonal	1.0 (37)	1.0 (18)	1.0 (1)	1.0 (27)	1.0 (32)	1.0 (25)
	> 100 *d*	27.0 (1)	52.0 (1)	52.0 (1)	52.0 (1)	52.0 (1)	52.0 (1)
	10–100 *d*	13.5 (2)	52.0 (1)	52.0 (1)	52.0 (1)	52.0 (1)	52.0 (1)
	6 *h*-10 *d*	2.0 (15)	2.0 (20)	2.0 (18)	3.0 (20)	2.0 (24)	3.0 (20)
	tide	1.0 (51)	1.0 (49)	1.0 (49)	1.0 (47)	1.0 (49)	1.0 (51)
	< 6 *h*	1.0 (51)	1.0 (50)	1.0 (52)	1.0 (51)	1.0 (49)	1.0 (50)

d and 10–100 *d components*, which are known to precondition floods (Pasarić and Orlić, 2001). In general, the duration of total extremes is shorter for 2–3 h than the duration of the 6 *h*-10 *d* extremes and approximately 1 h longer than the duration of *tide* and < 6 *h* extremes. As it was already suggested by our analysis, the < 6 *h component* is generally very weak (Fig. 11), and it is therefore unlikely that its duration significantly influences the duration of the total extremes. Consequently, the duration of positive and negative extremes is mostly governed by an interplay between *tide* and the 6 *h*-10 *d component*.

References

Androulidakis, Y.S., Kombiadou, K.D., Makris, C.V., Baltikas, V.N., Krestenitis, Y.N., 2015. Storm surges in the Mediterranean Sea: Variability and trends under future climatic conditions. Dynamics of Atmospheres and Oceans 71, 56–82. https://doi.org/10.1016/j.dynatmoce.2015.06.001.

Aucan, J., Ardhuin, F., 2013. Infragravity waves in the deep ocean: An upward revision. Geophysical Research Letters 40, 3435–3439. https://doi.org/10.1002/grl.50321.

Bajo, M., Međugorac, I., Umgiesser, G., Orlić, M., 2019. Storm surge and seiche modelling in the Adriatic Sea and the impact of data assimilation. Quarterly Journal of the Royal Meteorological Society 145, 2070–2084. https://doi.org/10.1002/qj.3544.

Bertotti, L., Bidlot, J.R., Buizza, R., Cavaleri, L., Janousek, M., 2011. Deterministic and ensemble-based prediction of Adriatic Sea sirocco storms leading to 'acqua alta' in Venice. Quarterly Journal of the Royal Meteorological Society 137, 1446–1466. https://doi.org/10.1002/qj.861.

Bouwer, L.M., Jonkman, S.N., 2018. Global mortality from storm surges is decreasing. Environmental Research Letters 13 (1), 014008. https://doi.org/10.1088/1748-9326/aa98a3.

Bubalo, M., Janeković, I., Orlić, M., 2021. Meteotsunami-related flooding and drying: numerical modeling of four Adriatic events. Natural Hazards 106 (2), 1–18. https://doi.org/10.1007/s11069-020-04444-4.

Burrage, D.M., Book, J.W., Martin, P.J., 2009. Eddies and filaments of the Western Adriatic Current near Cape Gargano: Analysis and prediction. Journal of Marine Systems 78, S205–S226. https://doi.org/10.1016/j.jmarsys.2009.01.024.

Caloi, P., 1938. Sesse dell'alto Adriatico con particolare riguardo al Golfo di Trieste. Memorie. R. Comitato Talassografico Italiano 247, 1–39.

Campetella, C.M., D'onofrio, E., Cerne, S.B., Fiore, M.E., Possia, N.E., 2007. Negative storm surges in the Port of Buenos Aires. International Journal of Climatology 27 (8), 1091–1101. https://doi.org/10.1002/joc.1452.

Canestrelli, P., Mandich, M., Pirazzoli, A.P., Tomasin, A., 2001. Venti, depressioni e sesse: perturbazioni delle maree a Venezia (1950–2000). Centro Previsioni e Segnalazione Maree, Città di Venezia, Venice, Italy.

Cavaleri, L., Bajo, M., Barbariol, F., Bastianini, M., Benetazzo, A., Bertotti, L., Chiggiato, J., Ferrarin, C., Trincardi, F., Umgiesser, G., 2020. The 2019 flooding of Venice and its implications for future predictions. Oceanography 33 (1), 42–49. https://doi.org/10.5670/oceanog.2020.105.

Cerovečki, I., Orlić, M., Hendershott, M.C., 1997. Adriatic seiche decay and energy loss to the Mediterranean. Deep-Sea Research I 44, 2007–2029. https://doi.org/10.1016/S0967-0637(97)00056-3.

Crisciani, F., Ferraro, S., Raicich, F., 1994. Interannual variability of the sea level at Trieste. Il Nuovo Cimento 17 (4), 377–384. https://doi.org/10.1007/BF02506725.

Cushman-Roisin, B., Gačić, M., Poulain, P.M., Artegiani, A., 2001. Physical Oceanography of the Adriatic Sea. Kluwer Academic Publishers, Dordrecht, Netherlands. https://doi.org/10.1007/978-94-015-9819-4.

Denamiel, C., Pranić, P., Quentin, F., Mihanović, H., Vilibić, I., 2020. Pseudo-global warming projections of extreme wave storms in complex coastal regions: the case of the Adriatic Sea. Climate Dynamics 55, 2483–2509. https://doi.org/10.1007/s00382-020-05397-x.

Dodet, G., Melet, A., Ardhuin, F., Bertin, X., Idier, D., Almar, R., 2019. The contribution of wind-generated waves to coastal sea level changes. Surveys in Geophysics 40, 1563–1601. https://doi.org/10.1007/s10712-019-09557-5.

Enriquez, A.R., Wahl, T., Marcos, M., Haigh, I.D., 2020. Spatial footprints of storm surges along the global coastlines. Journal of Geophysical Research Oceans, 125, e2020JC016367. https://doi.org/10.1029/2020JC016367.

Fenoglio-Marc, L., Kusche, J., Becker, M., 2006. Mass variation in the Mediterranean Sea from GRACE and its validation by altimetry, steric and hydrologic fields. Geophysical Research Letters 33, L19606. https://doi.org/10.1029/2006GL026851.

Fenoglio-Marc, L., Braitenberg, C., Tunini, L., 2012. Sea level variability and trends in the Adriatic Sea in 1993–2008 from tide gauges and satellite altimetry. Physics and Chemistry of the Earth 40–41, 47–58. https://doi.org/10.1016/j.pce.2011.05.014.

Ferrarin, C., Bajo, M., Benetazzo, A., Cavaleri, L., Chiggiato, J., Davison, S., Davolio, S., Lionello, P., Orlić, M., Umgiesser, G., 2021. Local and large-scale controls of the exceptional Venice floods of November 2019. Progress in Oceanography 197, 102628. https://doi.org/10.1016/j.pocean.2021.102628.

Ferrarin, C., Lionello, P., Orlić, M., Raicich, F., Salvadori, G., 2022. Venice as a paradigm of coastal flooding under multiple compound drivers. Scientific Reports 12 (1), 5754. https://doi.org/10.1038/s41598-022-09652-5.

Fukumori, I., Raghunath, R., Fu, L.L., 1998. Nature of global large-scale sea level variability in relation to atmospheric forcing: A modeling study. Journal of Geophysical Research Oceans 103, 5493–5512. https://doi.org/10.1029/97JC02907.

Goldberg, J., Kempni, K., 1938. On the sea level oscillations in Bakar Bay and on the problem of bay seiches in general (in Croatian). Prirodoslovna istraživanja Kraljevine Jugoslavije 21, 9–235.

Hamlington, B.D., Gardner, A.S., Ivins, E., Lenaerts, J.T.M., Reager, J.T., Trossman, D.S., Zaron, E.D., Adhikari, S., Arendt, A., Aschwanden, A., Beckley, B.D., Bekaert, D.P.S., Blewitt, G., Caron, L., Chambers, D.P., Chandanpurkar, H.A., Christianson, K., Csatho, B., Cullather, R.I., DeConto, R.M., Fasullo, J.T., Frederikse, T., Freymueller, J.T., Gilford, D.M., Girotto, M., Hammond, W.C., Hock, R., Holschuh, N., Kopp, R.E., Landerer, F., Larour, E., Menemenlis, D., Merrifield, M., Mitrovica, J.X., Nerem, R.S., Nias, I.J., Nieves, V., Nowicki, S., Pangaluru, K., Piecuch, C.G., Ray, R.D., Rounce, D.R., Schlegel, N.-J., Seroussi, H., Shirzaei, M., Sweet, W.V., Velicogna, I., Vinogradova, N., Wahl, T., Wiese, D.N., Willis, M.J., 2020. Understanding of contemporary regional sea-level change and the implications for the future. Reviews of Geophysics 58 (3), e2019RG000672. https://doi.org/10.1029/2019RG000672.

Hendershott, M.C., Speranza, A., 1971. Co-oscillating tides in long, narrow bays; the Taylor problem revisited. Deep-Sea Research 18, 959–980. https://doi.org/10.1016/0011-7471(71)90002-7.

Henderson, S.M., Bowen, A.J., 2003. Simulations of dissipative, shore-oblique infragravity waves. Journal of Physical Oceanography 33, 1722–1732. https://doi.org/10.1175/2398.1.

Hersbach, H., Bell, B., Berrisford, P., Hirahara, S., Horányi, A., Muñoz-Sabater, J., Nicolas, J., Peubey, C., Radu, R., Schepers, D., Simmons, A., Soci, C., Abdalla, S., Abellan, X., Balsamo, G., Bechtold, P., Biavati, G., Bidlot, J., Bonavita, M., Chiara, G., Dahlgren, P., Dee, D., Diamantakis, M., Dragani, R., Flemming, J., Forbes, R., Fuentes, M., Geer, A., Haimberger, L., Healy, S., Hogan, R.J., Hólm, E., Janisková, M., Keeley, S., Laloyaux, P., Lopez, P., Lupu, C., Radnoti, G., Rosnay, P., Rozum, I., Vamborg, F., Villaume, S., Thépaut, J.-N., 2020. The ERA5 global reanalysis. Quarterly Journal of the Royal Meteorological Society 146 (730), 1999–2049. https://doi.org/10.1002/qj.3803.

Hersbach, H., Bell, B., Berrisford, P., Biavati, G., Horányi, A., Muñoz Sabater, J., Nicolas, J., Peubey, C., Radu, R., Rozum, I., Schepers, D., Simmons, A., Soci, C., Dee, D., Thépaut, J-N., 2018. ERA5 hourly data on single levels from 1959 to present. Copernicus Climate Change Service (C3S) Climate Data Store (CDS), http://doi.org/10.24381/cds.adbb2d47, accessed: 20 September 2021.

Hinkel, J., Jaeger, C., Nicholls, R.J., Lowe, J., Renn, O., Peijun, S., 2015. Sea level rise scenarios and coastal risk management. Nature Climate Change 5, 188–190. https://doi.org/10.1038/nclimate2505.

Janeković, I., Kuzmić, M., 2005. Numerical simulation of the Adriatic Sea principal tidal constituents. Annales Geophysicae 23, 1–12. https://doi.org/10.5194/angeo-23-3207-2005.
Kânoğlu, U., Titov, V., Bernard, E., Synolakis, C., 2015. Tsunamis: bridging science, engineering and society. Philosophical Transactions of the Royal Society A 373, 20140369. https://doi.org/10.1098/rsta.2014.0369.
Kasumović, M., 1963. Long-period free oscillations in the Adriatic Sea (in Croatian). Rasprave Odjela za matematičke, fizičke i tehničke nauke JAZU, 2, 121–166.
Kulikov, E.A., Rabinovich, A.B., Spirin, A.I., Poole, S.L., Soloviev, S.L., 1983. Measurement of tsunami in the open ocean. Marine Geodesy 6, 311–329. https://doi.org/10.1080/15210608309379465.
Lahiri, S.N., 2003. Resampling methods for dependent data. Springer, New York. https://doi.org/10.1007/978-1-4757-3803-2.
Landerer, F.W., Volkov, D.L., 2013. The anatomy of recent large sea level fluctuations in the Mediterranean Sea. Geophysical Research Letters 40, 553–557. https://doi.org/10.1002/grl.50140.
Leder, N., Orlić, M., 2004. Fundamental Adriatic seiche recorded by current meters. Annales Geophysicae 22 (5), 1449–1464. https://doi.org/10.5194/angeo-22-1449-2004.
Leuliette, E.W., 2015. The balancing of the sea level budget. Current Climate Change Reports 1, 185–191. https://doi.org/10.1007/s40641-015-0012-8.
Lionello, P., Mufato, R., Tomasin, A., 2005. Sensitivity of free and forced oscillations of the Adriatic Sea to sea level rise. Climate Research 29, 23–39. https://doi.org/10.3354/cr029023.
Lionello, P., Galati, M.B., Elvini, E., 2012. Extreme storm surge and wind wave climate scenario simulations at the Venetian littoral. Physics and Chemistry of the Earth 40–41, 86–92. https://doi.org/10.1016/j.pce.2010.04.001.
Lionello, P., Conte, D., Reale, M., 2019. The effect of cyclones crossing the Mediterranean region on sea level anomalies on the Mediterranean Sea coast. Natural Hazards and Earth System Sciences 19, 1541–1564. https://doi.org/10.5194/nhess-19-1541-2019.
Lipizer, M., Partescano, E., Rabitti, A., Giorgetti, A., Crise, A., 2014. Qualified temperature, salinity and dissolved oxygen climatologies in a changing Adriatic Sea. Ocean Science 10, 771–797. https://doi.org/10.5194/os-10-771-2014.
Marcos, M., Tsimplis, M.N., Shaw, A.G.P., 2009. Sea level extremes in southern Europe. Journal of Geophysical Research 114, C01007. https://doi.org/10.1029/2008JC004912.
Marsooli, R., Lin, N., Emanuel, K., Feng, K.R., 2019. Climate change exacerbates hurricane flood hazards along US Atlantic and Gulf Coasts in spatially varying patterns. Nature Climate Change 10, 3785. https://doi.org/10.1038/s41467-019-11755-z.
Masina, M., Lamberti, A., 2013. A nonstationary analysis for the Northern Adriatic extreme sea levels. Journal of Geophysical Research Oceans 118, 3999–4016. https://doi.org/10.1002/jgrc.20313.
Međugorac, I., Pasarić, M., Orlić, M., 2015. Severe flooding along the eastern Adriatic coast: the case of 1 December 2008. Ocean Dynamics 65, 817–830. https://doi.org/10.1007/s10236-015-0835-9.
Međugorac, I., Pasarić, M., Pasarić, Z., Orlić, M., 2016. Two recent storm-surge episodes in the Adriatic. International Journal of Safety and Security Engineering 6 (3), 589–596. https://doi.org/10.2495/SAFE-V6-N3-589-596.
Međugorac, I., Orlić, M., Janeković, I., Pasarić, Z., Pasarić, M., 2018. Adriatic storm surges and related cross-basin sea level slope. Journal of Marine Systems 181, 79–90. https://doi.org/10.1016/j.jmarsys.2018.02.005.
Međugorac, I., Pasarić, M., Güttler, I., 2020. Will the wind associated with the Adriatic storm surges change in future climate? Theoretical and Applied Climatology 143, 1–18. https://doi.org/10.1007/s00704-020-03379-x.
Međugorac, I., Pasarić, M., Orlić, M., 2022a. Long-term measurements at Bakar tide-gauge station (east Adriatic). Geofizika 39 (1), 149–162. https://doi.org/10.15233/gfz.2022.39.8.
[dataset]Međugorac, I., Pasarić, M., Orlić, M., 2022b. Historical sea-level measurements at Bakar (east Adriatic). SEANOE. https://doi.org/10.17882/85171.
Medvedev, I., Vilibić, I., Rabinovich, A.B., 2020. Tidal resonance in the Adriatic Sea: Observational evidence. Journal of Geophysical Research Oceans, 125, e2020JC016168. https://doi.org/10.1029/2020JC016168.
Mel, R., Sterl, A., Lionello, P., 2013. High resolution climate projection of storm surge at the Venetian coast. Natural Hazards and Earth System Sciences 13, 1135–1142. https://doi.org/10.5194/nhess-13-1135-2013.
Menéndez, M., Woodworth, P.L., 2010. Changes in extreme high water levels based on a quasi-global tide-gauge data set. Journal of Geophysical Research Oceans 115, C10011. https://doi.org/10.1029/2009JC005997.
Merrifield, M.A., Genz, A.S., Kontoes, C.P., Marra, J.J., 2013. Annual maximum water levels from tide gauges: Contributing factors and geographic patterns. Journal of Geophysical Research 118, 2535–2546. https://doi.org/10.1002/jgrc.20173.
Mihanović, H., Vilibić, I., Carniel, S., Tudor, M., Russo, A., Bergamasco, A., Bubić, N., Ljubešić, Z., Viličić, D., Boldrin, A., Malačič, V., Celio, M., Comici, C., Raicich, F., 2013. Exceptional dense water formation on the Adriatic shelf in the winter of 2012. Ocean Science 9, 561–572. https://doi.org/10.5194/os-9-561-2013.
Mousavi, M.E., Irish, J.L., Frey, A.E., Olivera, F., Edge, B.L., 2011. Global warming and hurricanes: the potential impact of hurricane intensification and sea level rise on coastal flooding. Climatic Change 104, 575–597. https://doi.org/10.1007/s10584-009-9790-0.
Munk, W., Snodgrass, F., Carrier, G., 1956. Edge waves on the continental shelf. Science 123, 127–132. https://doi.org/10.1126/science.123.3187.127.
Neumann, B., Vafeidis, A.T., Zimmermann, J., Nicholls, R.J., Kumar, L., 2015. Future coastal population growth and exposure to sea level rise and coastal flooding – a global assessment. PLoS ONE 10 (3), e0118571. https://doi.org/10.1371/journal.pone.0118571.
Orlić, M., 2015. The first attempt at cataloguing tsunami-like waves of meteorological origin in Croatian coastal waters. Acta Adriatica 56 (1), 83–96. http://jadran.izor.hr/acta/pdf/56_1_pdf/56_1_4.pdf.
Orlić, M., Pasarić, M., 1994. Adriatic Sea level and global climate changes (in Croatian). Pomorski zbornik 32, 481–501.
Orlić, M., Pasarić, M., 2000. Sea level changes and crustal movements recorded along the east Adriatic coast. Il Nuovo Cimento C 23, 351–364. http://eprints.bice.rm.cnr.it/id/eprint/13924.
Orlić, M., Kuzmić, M., Pasarić, Z., 1994. Response of the Adriatic Sea to the bora and sirocco forcing. Continental Shelf Research 14, 91–116. https://doi.org/10.1016/0278-4343(94)90007-8.
Orlić, M., Belušić, D., Janeković, I., Pasarić, M., 2010. Fresh evidence relating the great Adriatic surge of 21 June 1978 to mesoscale atmospheric forcing. Journal of Geophysical Research Oceans 115, C06011. https://doi.org/10.1029/2009JC005777.
Orlić, M., Pasarić, M., Pasarić, Z., 2018. Mediterranean Sea-Level Variability in the Second Half of the Twentieth Century: a Bayesian Approach to Closing the Budget. Pure and Applied Geophysics 175, 3973–3988. https://doi.org/10.1007/s00024-018-1974-y.
Pasarić, M., Orlić, M., 2001. Long-term meteorological preconditioning of the North Adriatic coastal floods. Continental Shelf Research 21, 263–278. https://doi.org/10.1016/0278-4343(94)90007-8.
Pasarić, M., Pasarić, Z., Orlić, M., 2000. Response of the Adriatic Sea level to the air pressure and wind forcing at low frequencies (0.01–0.1 cpd). Journal of Geophysical Research 105, 11423–11439. https://doi.org/10.1029/2000JC900023.
Pérez Gómez, B., Vilibić, I., Šepić, J., Međugorac, I., Ličer, M., Testut, L., Fraboul, C., Marcos, M., Abdellaoui, H., Fanjul, E.A., Barbalić, D., Casas, B., Castaño-Tierno, A., Ćupić, S., Drago, A., Fraile, M.A., Galliano, D.A., Gauci, A., Gloginja, B., Guijarro, V. M., Jeromel, M., Revuelto, M.L., Lazar, A., Keskin, I.H., Medvedev, I., Menassri, A., Meslem, M.A., Mihanović, H., Morucci, S., Niculescu, D., de Benito, J.M.Q., Pascual, J., Palazov, A., Picone, M., Raicich, F., Said, M., Salat, J., Sezen, E., Simav, M., Sylaios, G., Tel, E., Tintoré, J., Zaimi, K., Zodiatis, G., 2022. Coastal sea level monitoring in the Mediterranean and Black seas. Ocean Science 18, 997–1053. https://doi.org/10.5194/os-18-997-2022.
Pirazzoli, P.A., 1987. Recent sea-level changes and related engineering problems in the lagoon of Venice (Italy). Progress in Oceanography 18 (1–4), 323–346. https://doi.org/10.1016/0079-6611(87)90038-3.
Pirazzoli, P.A., Tomasin, A., Ullmann, A., 2007. Extreme sea levels in two northern Mediterranean areas. Méditerranée – Revue géographique des pays méditerranées/Journal of Mediterranean Geography 108, 59–68. https://doi.org/10.4000/mediterranee.170.
Polli, S., 1959. La propagazione delle maree nell'Adriatico. IX Convegno della Associazione Geofisica Italiana, Associazione Geofisica Italiana, Roma 1959, 1–11.
Pugh, D., Woodworth, P.L., 2014. Sea level science. Cambridge, UK. Cambridge University Press. https://doi.org/10.1017/CBO9781139235778.
Pujol, M.I., Larnicol, G., 2005. Mediterranean sea eddy kinetic energy variability from 11 years of altimetric data. Journal of Marine Systems 58, 121–142. https://doi.org/10.1016/j.jmarsys.2005.07.005.
Rabinovich, A.B., 2009. Seiches and harbour oscillations. In: Kim, Y.C. (Ed.), Handbook of Coastal and Ocean Engineering. World Scientific, Singapore, pp. 193–236. https://doi.org/10.1142/6914.
Rabinovich, A.B., 2020. Twenty-seven years of progress in the science of meteorological tsunamis following the 1992 Daytona Beach event. Pure and Applied Geophysics 177 (3), 1193–1230. https://doi.org/10.1007/s00024-019-02349-3.
Raicich, F., 1996. On the fresh water balance of the Adriatic Sea. Journal of Marine Systems 9, 305–319. https://doi.org/10.1016/S0924-7963(96)00042-5.
[dataset]Raicich, F., 2019. Sea level observations at Trieste, Molo Sartorio, Italy. SEANOE. https://doi.org/10.17882/62758.
Raicich, F., Orlić., M., Vilibić, I., Malacic, V., 1999. A case study of the Adriatic seiches (December 1997). Il Nuovo Cimento C 22, 715–726.
Schwab, D.J., Rao, D.B., 1983. Barotropic oscillations of the Mediterranean and Adriatic Seas. Tellus 35 (1), 417–427. https://doi.org/10.1111/j.1600-0870.1983.tb00216.x.
Šepić, J., Orlić, M., Mihanović, H., 2022. Meteorological tsunamis in the Adriatic Sea – catalogue of meteorological tsunamis in Croatian coastal waters. Online, https://projekti.pmfst.unist.hr/floods/meteotsunamis; accessed: 26 September 2022.
Šepić, J., Orlić, M., Vilibić, I., 2008. The Bakar Bay seiches and their relationship with atmospheric processes. Acta Adriatica 49 (2), 107–123. https://hrcak.srce.hr/31813.
Šepić, J., Vilibić, I., Strelec Mahović, N., 2012a. Northern Adriatic meteorological tsunamis: observations, link to the atmosphere, and predictability. Journal of Geophysical Research: Oceans 117 (C2), C02002. https://doi.org/10.1029/2011JC007608.
Šepić, J., Vilibić, I., Jordà, G., Marcos, M., 2012b. Mediterranean sea level forced by atmospheric pressure and wind: variability of the present climate and future projections for several period bands. Global Planet. Change 86–87, 20–30. https://doi.org/10.1016/j.gloplacha.2012.01.008.
Šepić, J., Međugorac, I., Janeković, I., Dunić, N., Vilibić, I., 2016. Multi-meteotsunami event in the Adriatic Sea generated by atmospheric disturbances of 25–26 June 2014. Pure and Applied Geophysics 173 (12), 4117–4138. https://doi.org/10.1007/s00024-016-1249-4.
Stravisi, F., Ferraro, S., 1986. Monthly and annual mean sea levels at Trieste, 1890–1984. Bollettino di Oceanologia Teorica ed Applicata 4, 97–104.
Suzuki, T., Tatebe, H., 2020. Future dynamic sea level change in the western subtropical North Pacific associated with ocean heat uptake and heat redistribution by ocean

circulation under global warming. Progress in Earth and Planetary Science 7, 67. https://doi.org/10.1186/s40645-020-00381-9.
Tawn, J.A., Vassie, J.N., 1989. Extreme sea levels: The joint probability method revisited and revised. In: Proceedings of the Institution of Civil Engineers. https://doi.org/10.1680/iicep.1989.2975.
Thompson, P.R., Widlansky, M.J., Merrifield, M.A., Becker, J.M., Marra, J.J., 2019. A statistical model for frequency of coastal flooding in Honolulu, Hawaii, during the 21st century. Journal of Geophysical Research Oceans 124, 2787–2802. https://doi.org/10.1029/2018JC014741.
Thomson, R., Emery, W.J., 2014. Data Analysis Methods in Physical Oceanography: 3rd ed. Elsevier Science, New York. https://doi.org/10.1016/B978-0-444-50756-3.X5000-X.
Tosi, L., Teatini, P., Strozzi, T., 2013. Natural versus anthropogenic subsidence of Venice. Scientific Reports 3, 2710. https://doi.org/10.1038/srep02710.
Trigo, I.F., Davies, T.D., Bigg, G.R., 1999. Objective climatology of cyclones in the Mediterranean region. Journal of Climate 12 (6), 1685–1696. https://doi.org/10.1175/1520-0442(1999)012<1685:OCOCIT>2.0.CO;2.
Trigo, I.F., Davies, T.D., 2002. Meteorological conditions associated with sea surges in Venice: a 40 year climatology. International Journal of Climatology 22 (7), 787–803. https://doi.org/10.1002/joc.719.
Tsimplis, M.N., Blackman, D., 1997. Extreme sea-level distribution and return periods in the Aegean and Ionian Seas. Estuarine Coastal and Shelf Science 44, 79–89. https://doi.org/10.1006/ecss.1996.0126.
Tsimplis, M.N., Woodworth, P.L., 1994. The global distribution of the seasonal sea level cycle calculated from coastal tide gauge data. Journal of Geophysical Research 99, 16031–16039. https://doi.org/10.1029/94JC01115.
Tsimplis, M.N., Marcos, M., Perez, B., Challenor, P., Garcia-Fernandez, M.J., Raicich, F., 2009. On the effect of the sampling frequency of sea level measurements on return period estimate of extremes—Southern European examples. Continental Shelf Research 29, 2214–2221. https://doi.org/10.1016/j.csr.2009.08.015.
Ulbrich, U., Lionello, P., Belušić, D., Jacobeit, J., Knippertz, P., Kuglitsch, G., Leckebusch, G.C., Luterbacher, J., Maugeri, M., Maheras, P., Nissen, K.M., Pavan, V., Pinto, J.G., Saaroni, H., Seubert, S., Toreti, A., Xoplaki, E., Ziv, B., 2012. Climate of the Mediterranean: synoptic patterns, temperature, precipitation, winds, and their extremes. In: Lionello, P. (Ed.), the Climate of the Mediterranean Region - From the Past to the Future. Elsevier, Amsterdam, pp. 301–346. https://doi.org/10.1016/C2011-0-06210-5.
Unal, Y.S., Ghil, M., 1995. Interannual and interdecadal oscillation patterns in sea level. Climate Dynamics 11, 255–278. https://doi.org/10.1007/BF00211679.
Vilibić, 2006a. Seasonal sea level variations in the Adriatic. Acta Adriatica, 47(2), 141-158. https://hrcak.srce.hr/8506.
Vilibić, I., 2006b. The role of the fundamental seiche in the Adriatic coastal floods. Continent. Shelf Res. 26, 206–216. https://doi.org/10.1016/j.csr.2005.11.001.
Vilibić, I., Šepić, J., 2009. Destructive meteotsunamis along the eastern Adriatic coast: overview. Physics and Chemistry of the Earth 34, 904–917. https://doi.org/10.1016/j.pce.2009.08.004.
Vilibić, I., Šepić, J., 2010. Long-term variability and trends of sea level storminess and extremes in European Seas. Global and Planetary Change 71, 1–12. https://doi.org/10.1016/j.gloplacha.2009.12.001.
Vilibić, I., Šepić, J., 2017. Global mapping of nonseismic sea level oscillations at tsunami timescales. Scientific Reports 7, 40818. https://doi.org/10.1038/srep40818.
Vilibić, I., Orlić, M., Čupić, S., Domijan, N., Leder, N., Mihanović, H., Pasarić, M., Pasarić, Z., Srdelić, M., Strinić, G., 2005. A new approach to sea level observations in Croatia. Geofizika 22, 21–57. https://hrcak.srce.hr/136.
Vilibić, I., Šepić, J., Pasarić, M., Orlić, M., 2017. The Adriatic Sea: a long-standing laboratory for sea level studies. Pure and Applied Geophysics 174 (10), 3765–3811. https://doi.org/10.1007/s00024-017-1625-8.
Volkov, D.L., Landerer, F.W., 2015. Internal and external forcing of sea level variability in the Black Sea. Climate Dynamics 45, 2633–2646. https://doi.org/10.1007/s00382-015-2498-0.
Vousdoukas, M.I., Mentaschi, L., Voukouvalas, E., Verlaan, M., Feyen, L., 2017. Extreme sea levels on the rise along Europe's coasts. Earth's Future 5, 304–323. https://doi.org/10.1002/2016EF000505.
Wenzel, M., Schroter, J., 2007. The global ocean mass budget in 1993–2003 estimated from sea level change. Journal of Physical Oceanography 37, 203–213. https://doi.org/10.1175/JPO3007.1.
Wicks, A.J., Atkinson, D.E., 2017. Identification and classification of storm surge events at Red Dog Dock, Alaska, 2004–2014. Natural Hazards 86, 877–900. https://doi.org/10.1007/s11069-016-2722-1.
Wills, R.C.J., White, R.H., Levine, X.J., 2019. Northern Hemisphere stationary waves in a changing climate. Current Climate Change Reports 5, 372–389. https://doi.org/10.1007/s40641-019-00147-6.
Woodworth, P.L., 2017. Seiches in the Eastern Caribbean. Pure and Applied Geophysics 174, 4283–4312. https://doi.org/10.1007/s00024-017-1715-7.
Woollings, T., Barriopedro, D., Methven, J., Son, S.-W., Martius, O., Harvey, B., Sillmann, J., Lupo, A.R., Seneviratne, S., 2018. Blocking and its response to climate change. Current Climate Change Reports 4, 287–300. https://doi.org/10.1007/s40641-018-0108-z.
Yankovsky, A.E., 2009. Long-wave response of the West Florida Shelf to the landfall of Hurricane Wilma, October 2005. Journal of Coastal Research 24, 33–39. https://doi.org/10.2112/06-0824.1.
Zerbini, S., Raicich, F., Prati, C.M., Bruni, S., Del Conte, S., Errico, M., Santi, E., 2017. Sea-level change in the Northern Mediterranean Sea from long-period tide gauge time series. Earth-Science Reviews 167, 72–87. https://doi.org/10.1016/j.earscirev.2017.02.009.